Excitatory inputs to the hypothalamic paraventricular nucleus contribute to tonic, but not baroreflex, control of blood pressure in chronic kidney disease: possible role of angiotensin II and superoxide

Conor F. Underwood *(BMedSci)*

MACQUARIE University
SYDNEY·AUSTRALIA

October 2015

A thesis of the Department of Biomedical Sciences, Faculty of Medicine and Health Sciences, Macquarie University, submitted in fulfilment of the requirements for the degree of Master of Research.

Word count: 14,088

Figure/table count: 8/5

Supervisory panel

Prof. Jacqueline K. Phillips and Dr. Cara M. Hildreth

Department of Biomedical Sciences, Faculty of Medicine and Health Sciences, Macquarie University, Sydney, NSW, Australia.

Keywords

Chronic kidney disease, hypertension, baroreflex dysfunction, hypothalamic paraventricular nucleus, sympathetic nerve activity, superoxide, angiotensin II.

Financial declaration

This study was supported in part by the National Health and Medical Research Council of Australia Project grant (GNT1030301). During the course of this research CU was the recipient of a Macquarie University Research Training Pathway Scholarship. The research was otherwise conducted in the absence of any commercial or financial relationships.

Declaration of originality

I hereby declare that the work presented in this thesis has not been submitted for a higher degree to any other university or institution. To the best of my knowledge this submission contains no material previously published or written by another person, except where due reference is stated otherwise. Any contribution made to the research by others is explicitly acknowledged.

Conor F. Underwood

Student number: 42104068

Department of Biomedical Sciences

Faculty of Medicine and Health Sciences

Macquarie University

Date of submission

9/10/2015

Declaration of contributions

JK Phillips and CM Hildreth contributed to the concept and experimental design of the research project and assisted with the review of this thesis. Ms Rochelle Boyd performed coverslipping of the brain sections as detailed for Study 2.

Acknowledgements

To my parents, I am forever grateful for the ongoing support and opportunities you have provided me with during my education. To my partner, Caitlyn, thank you for enduring my absence during the early starts, late finishes and weekend urine collections. I also wish to thank my valued mentors, Jackie and Cara, for dedicating their time and resources to train me; for driving me to always achieve more; and above all for fostering my passion for autonomic neuroscience. I am grateful for the technical assistance provided by Rochelle and other departmental members.

Abstract

Increased cardiovascular mortality in chronic kidney disease (CKD) is in part due to hypertension and impaired baroreflex regulation of blood pressure. We tested the hypothesis that increased glutamatergic drive of the paraventricular nucleus (PVN) contributes to hypertension and baroreflex dysfunction in the Lewis Polycystic Kidney rat (LPK) model of CKD. In urethane anaesthetised adult male Lewis control and LPK rats (n=13) instrumented to record arterial pressure, heart rate (HR) and renal sympathetic nerve activity (RSNA), bilateral PVN microinjections of the glutamate receptor antagonist kynurenic acid (100mM) reduced systolic blood pressure to a greater extent in LPK vs. Lewis (-31±3 vs. -10±3mmHg P<0.01), did not influence HR in either strain (P>0.05) and transiently increased RSNA in LPK rats only (5 min post-microinjection 119±2 vs. baseline 100±1% P<0.05). Baroreflex curves for HR and RSNA were rightward shifted in LPK and gain was reduced vs. Lewis, however kynurenic acid did not influence baroreflex parameters in either strain (both P>0.05). Considering that angiotensin II-mediated superoxide production may facilitate excitation within the PVN, we assessed PVN superoxide in-situ with the redox-sensitive fluorophore dihydroethidium (DHE) in adult mixed-sex Lewis and LPK rats (n=22) that were untreated or treated with the angiotensin II AT_1 receptor antagonist losartan (30mg/kg/day) from 4 weeks of age. In untreated rats, PVN DHE fluorescence was greater in LPK vs. Lewis (2.0±0.3 vs. 1.0±0.2 relative fluorescence P=0.02), but was normalised by losartan (1.3±0.1). These data suggest that enhanced PVN glutamatergic activity maintains hypertension in LPK but not baroreflex dysfunction, and implicate AT_1 receptor-dependent superoxide overproduction as a possible mechanism.

Contents

1. Introduction

Autonomic control of the circulation is necessary to distribute cardiac output to the peripheral tissues in keeping with current physiological and environmental demands whilst also preserving arterial pressure within narrow limits. The heart and vasculature are richly innervated by autonomic efferents that exhibit a level of activity that is tonic at rest and continually modulated to rapidly adjust arterial pressure (Thomas, 2011). The intrinsic pacemaker activity of the heart is regulated by the opposing actions of cardiac vagal (parasympathetic) and sympathetic efferents that negatively and positively influence heart rate (HR), respectively (Ng et al., 2001). Importantly, however, these two classes of cardiac autonomic efferents are not simply mutually exclusive opposites, but share a unique interaction at the level of the heart that facilitates vagal predominance (Brack et al., 2004). Sympathetic outflow to the resistance vessels positively influences vasomotor tone and is the major determinant of peripheral vascular resistance at rest (Guyenet, 2006). Over longer-timescales, sympathetic innervation of the kidneys is an important determinant of blood pressure, positively influencing blood volume and arterial pressure by reducing renal blood flow, promoting sodium reabsorption and stimulating the secretion of renin, the rate limiting enzyme of the circulating renin-angiotensin hormone system (RAS) (Hollenberg, 1999; DiBona, 2005). Autonomic control of the circulation is coordinated by a network of neurons in the brainstem and hypothalamus that appropriately keep pace with homeostatic demands in health, however may function maladaptively in various disease states (Huang et al., 2014; Moraes et al., 2014).

Chronic kidney disease (CKD) is defined as a progressive and irreversible decline in renal function (Levey et al., 2005). However it is clear individuals with CKD are more likely to develop cardiovascular disease and die before renal replacement therapy (i.e. haemodialysis or renal transplant) is necessitated (Keith et al., 2004). Heightened cardiovascular risk in CKD involves the cumulative effect of highly prevalent traditional cardiovascular risk factors (e.g. hypertension, diabetes and dyslipidaemia) and CKD-specific risk factors (e.g. uraemia, proteinuria and anaemia) (Menon et al., 2005; van der Velde et al., 2011). Of note, hypertension develops with a high prevalence in the CKD patient population (Cheng et al., 2008), serving to independently inflate cardiovascular risk (Franklin and Wong, 2013) and promote the progression of CKD towards end-stage renal disease (Klahr et al., 1994; Tozawa et al., 2003). As a factor likely implicated in hypertension and cardiac remodelling (Siddiqi et al., 2010), sympathetic activity is upregulated in CKD, with evidence that patients have augmented plasma noradrenaline (Ishii et al., 1983) as well as greater burst activity of whole sympathetic fibres innervating muscle vascular beds (Klein et al., 2003a; Grassi et al., 2011). Angiotensin II (Ang II), an integral vasoactive, anti-natriuretic and centrally-acting neuromodulator peptide of the RAS (Wright and Harding, 2013), also plays an important role in the pathogenesis of CKD, with this being underscored by the efficacy of pharmacological Ang II inhibition in improving cardiovascular prognosis (Balamuthusamy et al., 2008) and reducing sympathetic hyperactivity within the CKD patient population (Klein et al., 2003b).

Autonomic dysfunction manifests in CKD not only as an inappropriately high level of sympathetic nerve activity (SNA), but also impaired cardiovascular reflex function. The arterial baroreceptor reflex (baroreflex) is an autonomic reflex responsible for maintaining arterial pressure within a narrow range by modulating cardiac vagal and sympathetic outflows. As a clinical marker of cardiac vagal function (Swenne, 2013), heart rate baroreflex sensitivity progressively declines with deteriorating renal function in CKD (Bavanandan et al., 2005; Lacy et al., 2006). Indeed, impaired control of the cardiac vagus is well documented in CKD, with this patient population exhibiting an overall reduction in HR variability (Chandra et al., 2012) and reduced HR responses to respiration and the Valsalva maneuver (Agarwal et al., 1991).

Reduced baroreflex sensitivity accelerates the progression of cardiovascular disease (La Rovere et al., 1988; Mortara et al., 1997), and within the CKD patient population positively predicts the risk of sudden cardiac and all-cause mortality (Johansson et al., 2007; John et al., 2008). In contrast to cardiac vagal baroreflex function, which has been consistently reported as reduced, whether baroreflex control of SNA is impaired in CKD is less clear, with baroreflex control of muscle SNA reported as reduced (Tinucci et al., 2001) or alternatively normal (Ligtenberg et al., 1999) in humans with CKD. Nevertheless, the pathogenesis of baroreflex dysfunction in CKD is not well defined.

The baroreflex operates through a feedback loop comprising of peripheral sensory and autonomic effector components that are bridged by a core network of neurons in the medulla (Figure 1) (Pilowsky and Goodchild, 2002). The afferent limb of the baroreflex, the arterial baroreceptors, are mechanosensitive neurons located within the vascular wall of the carotid sinus and aortic arch that relay arterial pressure information to circuits within the medulla responsible for generating cardiac vagal and sympathetic outflows (Krauhs, 1979; Guyenet, 2006). Baroreceptor afferents have a discharge pattern characterised by tonic activity at a resting level of arterial pressure that increases in parallel with rising arterial pressure to a saturation point (baroreceptor loading) and is progressively silenced below baseline activity with falling arterial pressure (baroreceptor unloading) (Grimm, 1997). The level of arterial baroreceptor activity at rest provides a fundamental source of excitatory drive to cardiac vagal efferents as well as inhibitory control over barosensitive sympathetic efferents that is enhanced or withdrawn in response to baroreceptor loading and unloading, respectively (McAllen and Spyer, 1978; Guyenet, 2006).

The initial synapse for carotid and aortic baroreceptors entering the central nervous system (CNS) via the glossopharyngeal and vagus nerves (equivalent to the carotid sinus and aortic depressor nerves in the rat), respectively, is the nucleus of the solitary tract (NTS) (Aviado and Schmidt, 1955; Loewy, 1990). Baroreflex control of the cardiac vagus involves an excitatory circuit mediated by the activation of cardiac vagal preganglionic neurons in the nucleus ambiguus by second- or higher-order NTS neurons (McAllen and Spyer, 1978; Blinder et al., 1998). In contrast, baroreflex control of SNA involves a circuit that operates by restraining tonically generated sympathetic outflow through disinhibition. This involves reflex activation of a group of GABAergic interneurons in the caudal ventrolateral medulla (CVLM) by second- or higher-order barosensitive NTS neurons that in turn inhibit presympathetic neurons in the rostral ventrolateral medulla (RVLM) (Blessing, 1988; Agarwal et al., 1990; Jung et al., 1991). In addition to this fundamental medullary relay circuit, neurons within the hypothalamic paraventricular nucleus (PVN) receive afferent baroreceptor input (Ciriello and Calaresu, 1980a; Ciriello and Caverson, 1984), and can produce neurohumoral changes (Leng et al., 1999; Chen and Toney, 2010) as well as modulate the activity of the medullary baroreflex circuit (Kubo and Kihara, 1990; Higa et al., 2002).

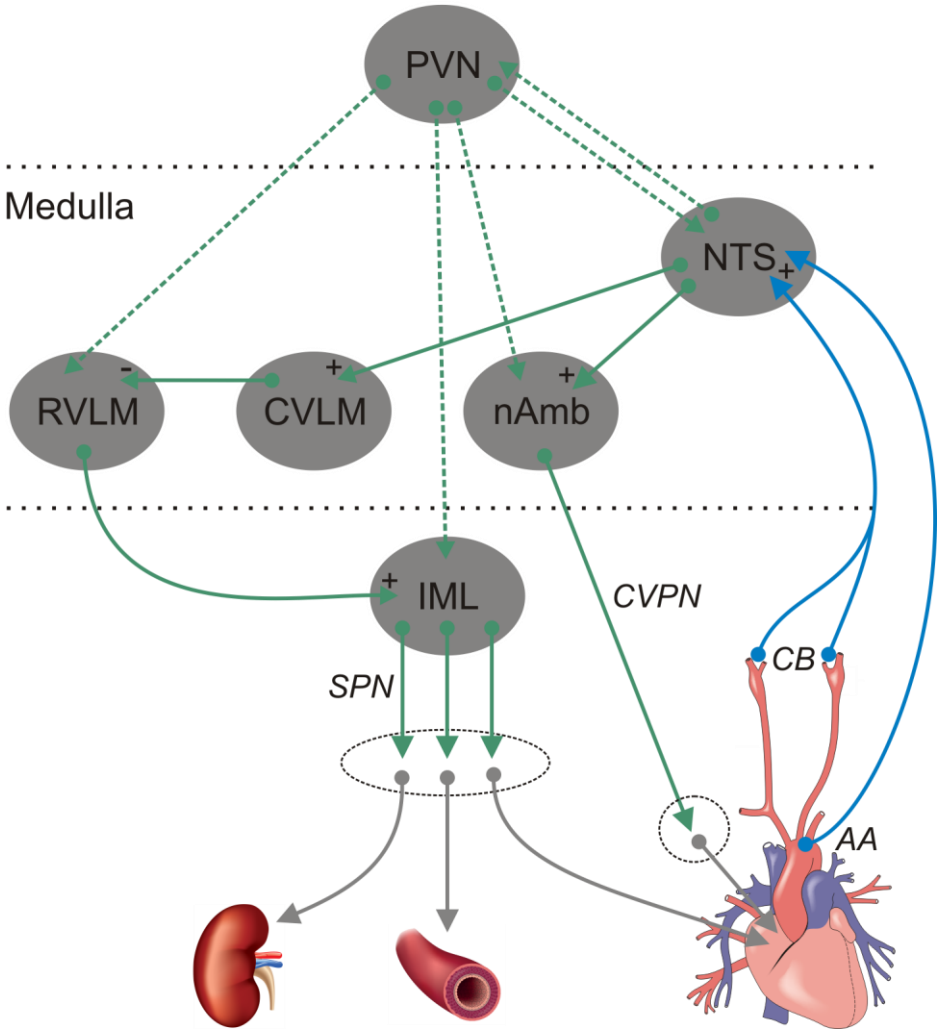

Figure 1: Schematic illustration of the baroreflex pathway showing peripheral sensory neurons (blue), central neurons (green) and peripheral autonomic efferents (grey). Baroreceptor afferents located in the aortic arch (AA) and carotid body (CB) transduce arterial pressure and transmit this information to the nucleus of the solitary tract (NTS). Barosensitive NTS neurons are a source of excitatory drive of cardiac vagal preganglionic neurons (CVPN) with cell bodies located in the nucleus ambiguus (nAmb). Post ganglionic cardiac vagal neurons innervate the heart and negatively influence heart rate. Barosensitive NTS neurons also provide excitatory input to GABAergic interneurons in the caudal ventrolateral medulla (CVLM) that inhibit presympathetic neurons in the rostral ventrolateral medulla (RVLM). The activity of presympathetic RVLM neurons drives the activity of sympathetic preganglionic neurons (SPN) in the intermediolateral spinal cord (IML). Post-ganglionic SPNs innervate the kidneys, vasculature and heart. The paraventricular nucleus of the hypothalamus (PVN) is an accessory site of the central baroreflex circuitry known to receive baroreceptor input from the NTS and project to sites within the primary baroreflex circuits, including the NTS, nAmb, RVLM and IML. Afferent and efferent PVN pathways are shown as green dashed lines. Predominately excitatory and inhibitory pathways of the primary baroreflex circuit are indicated by + and –, respectively. Peripheral ganglia are indicated as dashed black circles.

The Lewis Polycystic Kidney rat (LPK) is an established model of CKD that develops a complex disease phenotype similar to that of human autosomal recessive polycystic kidney disease (PKD) (Phillips et al., 2007). Renal disease arises in the LPK from corticomedullary cysts resulting from a single point mutation in the never in mitosis gene A-related kinase 8

(Nek8) gene (McCooke et al., 2012). The time-course of renal functional loss in the LPK occurs in parallel with renal cystic expansion, inflammation and fibrosis (Phillips et al., 2007; Jeewandara et al., 2015). The first evidence of renal cysts occurs at 3 weeks of age alongside elevated serum urea. By 12 weeks of age, average cyst diameter has doubled, uraemia is more severe, and other haematological and urinological markers of impaired renal function, including elevated serum creatinine and proteinuria, are present (Phillips et al., 2007). In addition to the primary renal pathology, the LPK develops several cardiovascular abnormalities, including hypertension, presenting at 6 weeks of age before renal function is significantly compromised, cardiac hypertrophy and fibrosis, and vascular calcification and remodelling (Phillips et al., 2007; Ng et al., 2011b; Jeewandara et al., 2015).

Similar to human PKD (Klein et al., 2001), the LPK develops autonomic dysfunction. Evidence from anaesthetised and conscious preparations have shown that by 12 weeks of age LPK exhibit impaired baroreflex control of HR and SNA, as well as elevated sympathetic vasomotor tone (Hildreth et al., 2013; Salman et al., 2014; Yao et al., 2015). Previous studies have provided insight into where in the baroreflex neuroaxis dysfunction arises in the LPK. Early in the disease course in 8 week old male LPK the ability of the aortic depressor nerve to transduce arterial pressure is impaired, despite baroreflex function being largely maintained at this age (Salman et al., 2014). This baroreceptor afferent deficit in male LPK persists with the onset of overt baroreflex dysfunction at 12 weeks of age, and most likely arises secondary to vascular remodelling (Salman et al., 2014). Importantly, however, loss of baroreflex function in 12 week old LPK involves a central impairment since the ability of direct aortic depressor nerve stimulation to reflexively decrease HR and renal SNA (RSNA) is significantly reduced at 12 weeks relative to age-matched healthy Lewis and 8 week old LPK rats (Salman et al., 2014). This suggests therefore that baroreflex dysfunction arises in male LPK from deficits in both afferent and central components of the reflex arc. While the former presents early in the disease course before baroreflex function is overtly compromised, development of the latter appears to be necessary for the full expression of baroreflex dysfunction.

The PVN exerts control over autonomic function through an efferent projection pattern that includes several sites involved in the tonic and baroreflex control of autonomic outflow, including the NTS, nucleus ambiguus, RVLM and preganglionic sympathetic neurons in the intermediolateral spinal cord (IML) (Buijs, 1978; Swanson and Kuypers, 1980; Stuesse and Fish, 1984; Shafton et al., 1998; Affleck et al., 2012) (Figure 1). The activity of PVN projection neurons depends on a balance between excitatory ionotropic glutamate receptors and inhibitory ionotropic GABA receptors (Li et al., 2006). When this balance favours excitation, such as following an acute peripheral hyperosmotic stimulus (Antunes et al., 2006), a pressor, tachycardic and sympathoexcitatory response is elicited (Li et al., 2006). Excitatory/inhibitory balance within the PVN also responds chronically to Ang II, with evidence from patch-clamp recordings of PVN neurons showing that responses to activation of the iontropic glutamate NMDA receptor are enhanced in mice chronically treated with low dose Ang II (Wang et al., 2013). Importantly this enhancement of NMDA receptor signalling in PVN neurons in Ang II treated mice is abolished in the presence of a superoxide scavenger, suggesting a critical role of reactive oxygen species (ROS) production. In fact, ROS production within the PVN appears obligatory for the full expression of hypertension and sympathetic hyperactivity resulting from chronic Ang II treatment (Su et al., 2014).

Elevated excitatory drive of the PVN is postulated to contribute to hypertension and autonomic dysfunction in CKD. In support of this, studies examining the expression of the immediate-early gene c-Fos, a marker of chronic neuronal activity, have revealed that the PVN is activated in adult LPK rats (Ang et al., 2007). Moreover, glutamatergic drive of the PVN is enhanced in

CKD, with preliminary evidence from our laboratory that microinjection of the non-specific ionotropic glutamate receptor antagonist kynurenic acid within the PVN produces a greater decrease in blood pressure and lumbar SNA in LPK compared to Lewis rats (Hildreth and Phillips, 2014). However, currently it is unknown whether elevated glutamatergic tone of the PVN mediates an increase in sympathetic outflow to other vascular beds in CKD. Furthermore, while it is known that ROS production within the CNS is required to elicit pressor and sympathoexcitatory responses in rats with phenol-induced acute renal injury (Ye et al., 2006), whether increased ROS signalling within the PVN is feature of CKD is unknown, as is the role of Ang II.

The main aim of this study was to determine whether elevated glutamatergic activity within the PVN contributes to baroreflex dysfunction in the LPK. To this end, we compared baroreflex control of HR and RSNA in anaesthetised LPK and Lewis animals in response to microinjection of kynurenic acid into the PVN. To gain insight into the mechanism driving altered neural activity within the PVN in CKD, we examined the hypothesis that ROS production within the PVN would be greater in LPK than Lewis rats, and that this would be reduced by chronic treatment with the AT_1 receptor antagonist losartan.

2. Methods

2.1 Animals and experimental groups

Lewis and LPK rats were obtained from the Animal Resource Centre, Murdoch, Western Australia, Australia. Animals were group housed in standard living conditions with a 12 hour light/dark cycle and access to standard rodent chow and tap water *ad libitum*. Experiments were performed in accordance with The Australian Code of Practice for the Care and Use of Animals (8th edition, 2013) and were approved by the Macquarie University Animal Ethics Committee (protocol number 2015/001).

Two separate experimental groups were used. In study 1, male adult (13-14 weeks) Lewis (*n*=8) and LPK (*n*=8) rats were used for acute microinjection experiments. In study 2, mixed-sex adult (12-14 weeks) Lewis (*n*=9) and LPK (*n*=13) rats were used to evaluate AT_1 receptor-dependent production of superoxide within in the PVN.

2.2 Study 1: PVN microinjection and assessment of baroreflex function

2.2.1 Assessment of renal function

Animals were acclimatised to metabolic cages in the week prior to acute microinjection experiments. Approximately 24-72 h prior to the experiment, animals were placed in a metabolic cage for 4 h to obtain a urine sample. Arterial blood (0.3-0.4 ml) was collected from the deep femoral artery during the non-recovery microinjection experiment. The sample was immediately centrifuged to separate plasma (IDEXX StatSpin, IDEXX laboratories Pty Ltd., NSW, Australia). Urine and plasma samples were stored at -80°C until analysis. A VetTest chemistry analyser (IDEXX laboratories Pty Ltd.) was used to measure urinary concentrations of protein and creatinine and plasma concentrations of urea and creatinine.

2.2.2 Surgical preparation

Animals were anaesthetised with ethyl carbamate (urethane 10% w/v in 0.9% saline; 1.3 g/kg i.p., Sigma Aldrich, Australia). Depth of anaesthesia was assessed by the absence of noxious tactile and corneal reflexes, and when required maintenance doses of urethane (65-130 mg/kg i.p. or i.v.) were administered. Body temperature was assessed with a digital rectal thermometer (Harvard Apparatus, MA, USA) and maintained at 37±0.5℃ with a thermostatically controlled heating mat (Harvard Apparatus) and manually operated heat-lamp.

All animals underwent the following surgical procedures:

Arterial and venous cannulation: The left deep femoral artery and both deep femoral veins were cannulated to record arterial pressure and to administer intravenous fluids (Hartmann's solution 5 ml/kg/hr) and drugs respectively. Briefly, an incision was made along the inner hind-leg and superficial adipose tissue removed to expose the femoral vessels. The femoral vein and artery were then visualised and separated. The left femoral artery and both femoral veins were cannulated with polyethylene tubing (inner diameter 0.58 mm and outer diameter 0.96 mm) and secured in place with silk suture. Arterial cannulas were prefilled with heparinised saline (5 IU/ml 0.9% saline) and venous cannulas with normal 0.9% saline. The arterial cannula was attached to a pressure transducer and the pressure signal was acquired with a CED 1401 plus (Cambridge Electronic Designs Ltd., Cambridge, UK) and Spike2 software (v7, Cambridge Electronic Designs Ltd., Cambridge, UK). Heart rate was extracted from the arterial pressure signal in real-time.

Tracheostomy: A midline incision was made along the ventral surface of the neck and the sternohyoid muscles retracted to visualise the trachea. A small hole was made in the trachea and a 14G catheter was inserted and secured in place with silk suture. Animals were mechanically ventilated with oxygen enriched room air (1 ml/100g body weight at 65±5 cycles per minute; adjusted to maintain arterial pCO_2 40±5 mmHg and pH 7.4±0.5 as measured with a VetStat blood gas analyser; IDEXX laboratories Pty Ltd.) and paralysed with cisatracurium (6 mg/kg/hr i.v., GlaxoSmithKline Pty Ltd, Victoria, Australia).

Renal sympathetic nerve recording: A dorsal flank incision was made to access the retroperitoneal cavity and expose the left kidney. The intersection of the left renal artery and abdominal aorta was separated from the surrounding adipose tissue and fascia and a branch of the left renal nerve was dissected free from fascia and adventitia of the aorta and left renal artery, cut at its proximal end, immersed in paraffin oil and mounted onto a silver bipolar recording electrode. Renal nerve branches were typically found coursing alongside or across the aorta towards the renal artery. The nerve signal was band-pass filtered (30-1000 Hz), amplified with a bio-amplifier (2000x; CWE Inc., Ardmore, PA, USA) and sampled at 5 kHz with a CED 1401 plus and Spike2 software (Cambridge Electronic Designs Ltd.). The presence of both pulse modulation and a reduction in SNA after a pressor dose of phenylephrine (PE; 50 µg/ml 0.9% saline i.v., Sigma Aldrich) was used to verify the validity of the renal sympathetic nerve recording. In *n*=1 Lewis, RSNA was not recorded.

Brain exposure: Animals were positioned in a stereotaxic frame and placed in the flat skull position with bregma and true lambda equidistant in the vertical plane. A burr hole approximately 10 mm in diameter was made in the skull approximately 1 mm caudal to bregma and centered on the midline of the skull.

Following completion of all surgical procedures, the preparation was stabilised for at least 30 min before the initiation of the experimental protocol.

2.2.3 Experimental procedures

2.2.3.1 Assessment of baroreflex function

Baroreflex function was assessed before and 30 min after PVN microinjection. This was achieved by first decreasing systolic blood pressure (SBP) to 50-80 mmHg over a period of 20-40 sec with sodium nitroprusside (SNP; 50 µg/ml; 15-20 µg/min in 0.9% saline i.v., Sigma Aldrich), allowing for HR and RSNA responses to plateau. SBP was then increased slowly to ~200-230 mmHg in Lewis and ~300-330 mmHg in LPK by terminating the infusion of SNP and infusing PE at increasing rates (50 µg/ml; 5-20 µg/min in 0.9% saline i.v., Sigma Aldrich) into the other femoral vein as previously described (Cassaglia et al., 2014). In *n*=2 Lewis and *n*=2 LPK, SNP (30-50 µg/kg) and PE (30-50 µg/kg) were infused separately over a 40-60 sec period, obtaining a stable baseline between sequential infusions. Drug infusions were achieved with an infusion pump (Havard Apparatus, MA, USA). Two to three replicate curves were generated before and after PVN microinjection.

2.2.3.2 PVN microinjection

Kynurenic acid (100 nl, 100 mM, Sigma Aldrich) was microinjected into the PVN bilaterally (1.4-1.6 mm caudal to bregma, 0.4-0.5 mm lateral to the midline and 8.0 mm ventral to the surface of the dura as outlined by Paxinos and Watson (2013)) using a pre-calibrated micropipette (barrel inner diameter 0.25 mm and outer diameter 1 mm) connected to a syringe with silastic tubing. We elected to use kynurenic acid to non-selectively block ionotropic

glutamate receptors since, within the PVN, both NMDA and non-NMDA receptors are involved in autonomic control (Li et al., 2006), and it is currently unknown if ionotropic glutamate receptor subtypes within the PVN are differentially involved in the modulation of baroreflex function. Kynurenic acid was prepared by dissolving the drug in the smallest possible volume of 1 M NaOH and titrating the solution with 1 M HCL and 1 M NaOH to achieve pH 7.2-7.4. The solution was then diluted with phosphate-buffered saline (PBS; pH 7.4; 137 mM NaCl, 2.7 mM KCl, 10 mM phosphate buffer) to achieve a final 100 mM concentration of kynurenic acid. At the end of the experiment, animals were euthanised with sodium pentobarbital (65 mg in 0.9% saline i.v., Virbac Pty Ltd, NSW, Australia) and a death level of RSNA was obtained. Thereafter injection sites were marked with a saturated solution of pontamine sky blue dye. In *n*=4 Lewis and *n*=5 LPK, injection sites were also marked with FluoroMax fluorescent polystyrene microbeads (1/10,000; Thermo Fisher Scientific, CA, USA) that were co-injected with kynurenic acid during the experiment. Forebrains were stored in 10% neutral buffered formalin for at least 12 h before being sectioned at 100 µm with a vibrating microtome (Leica VT1200s, Leica Microsystems Pty Ltd., NSW, Australia). To facilitate anatomical mapping of injection sites, sections were stained with cresyl violet (0.1% cresyl violet acetate; Sigma Aldrich) for 6-8 min, serially dehydrated (ethanol; 50%, 70%, 95% and 100%) and coverslipped. Sections were imaged with a conventional microscope (Zeiss Axioimager.Z1, Carl Zeiss Microscopy, NSW, Australia) and mapped onto the rat brain atlas (Paxinos and Watson, 2013) using CorelDRAW Graphics Suite X4 software (Corel Corporation, Ontario, Canada). Representative forebrain sections marked with pontamine sky blue dye and fluorescent microbeads are shown in Figure 2. Although the location of pontamine sky blue dye marked sites largely conformed to those marked with fluorescent microbeads, if the location of these markers differed then fluorescent microbeads were used to determine the anatomical location of the microinjection site.

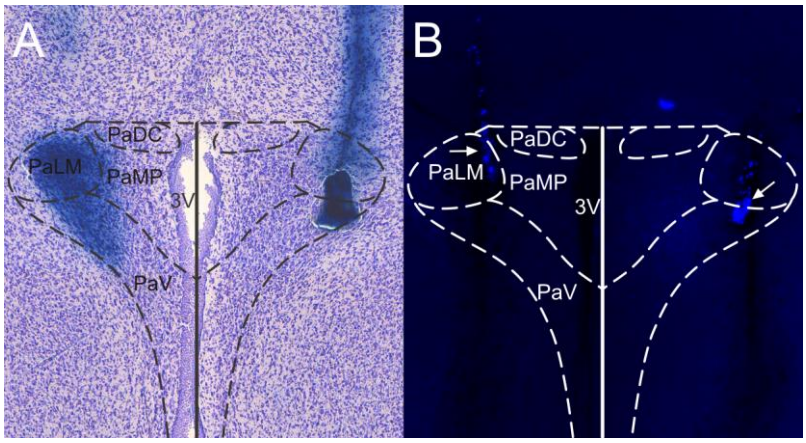

Figure 2: Representative forebrain sections showing microinjection sites within the paraventricular nucleus of the hypothalamus (PVN) marked with **(A)** pontamine sky blue dye in a Lewis rat and **(B)** fluorescent microbeads (indicated as arrows) in another Lewis rat. The forebrain section is stained with cresyl violet in **(A)**. The anatomical boarder of the PVN is outlined. PaMP, paraventricular nucleus medial parvocellular; 3V, third ventricle; PaV, paraventricular nucleus ventral part; PaDC, paraventricular nucleus dorsal cap; PaLM, paraventricular nucleus lateral magnocellular.

2.2.4 Data analysis

All data was analysed offline using Spike2 software. Systolic blood pressure (SBP) and diastolic blood pressure (DBP) were determined from the peak and trough amplitudes of the

arterial pressure waveform, respectively. Pulse pressure (PP) was calculated as the difference between SBP and DBP, and mean arterial pressure (MAP) as the 1 sec average of the AP waveform. HR was computed from the frequency of arterial pressure waveform peaks. The RSNA waveform was rectified, smoothed (1 sec constant) and corrected for background noise by subtracting a death level of RSNA activity. RSNA was then normalised to the 60 sec period immediately prior to PVN microinjection, setting this as 100% and the level of RSNA following euthanasia 0%.

2.2.4.1 Baseline parameters

Baseline measurements of MAP, SBP, DBP, PP, HR and RSNA (μV) were taken over a 5 min period immediately prior to microinjection.

2.2.4.2 Time-course changes in arterial pressure, HR and RSNA in response to PVN microinjection

MAP, SBP, DBP, PP, HR and RSNA (% of baseline) were averaged into 5 min bins for the 30 min period following microinjection.

2.2.4.3 Assessment of baroreflex control of HR and RSNA

To derive baroreflex function curves, Spike2 was used to generate an x-y plot of HR (bpm) and RSNA (%) against SBP. Plots were constructed from the trough of the SNP curve over the slow rising phase of the PE pressor curve. In those experiments (n=2 Lewis and n=2 LPK) where sodium nitroprusside and phenylephrine infusions were separated by a stable baseline, curves were constructed during the falling phase of the sodium nitroprusside depressor curve and the rising phase of the phenylephrine pressor curve. Each individual curve was exported into Excel 2013 (Microsoft Office, Microsoft Corporaton, WA, USA) and the level of HR (bpm) and RSNA (%) averaged into 10 mmHg bins across the blood pressure range of each curve. Averaged data points were fitted to a four-parameter sigmoid regression curve using GraphPad Prism software (GraphPad Prism software v6 Inc., La Jolla, CA, USA) and the following equation:

$$y = \frac{A_1}{1 + \exp[A_2(SBP - A_3)]} + A_4$$

where A_1 is the y-axis range of the curve, A_2 is the gain coefficient, A_3 the midpoint of the curve and A_4 is the lower plateau. These values were used to calculate the range of the reflex, SBP saturation (SBP_{sat}), SBP threshold (SBP_{thr}) and SBP operational range as previously described (Kent et al., 1972).

All curves used in the final analysis had an R^2 value greater than 0.98. In *n*=1 Lewis and *n*=2 LPK, HR curves could not be fitted to the sigmoidal curve and were excluded from the final analysis. Each individual curve was generated over a fixed range of 50-250 mmHg for Lewis and 50-350 mmHg for LPK, reflecting the physiological range over which pressor and depressor responses were elicited in each strain. Baseline and post microinjection curves were averaged for each strain.

2.2.5 Statistical analysis

All data are expressed as mean ± standard error of the mean (SEM). GraphPad Prism was used for statistical analysis. To detect strain differences in baseline parameters an unpaired t-test was

used. A repeated measures two-way ANOVA with Bonferoni post-hoc test was used to detect differences within and between strains in response to PVN microinjection. We did not perform statistical analysis on urinary protein parameters since urinary protein was below the threshold of detection in Lewis rats. A Grubb's test (α=0.05) was used to identify outliers for HR and RSNA responses to PVN microinjection. A threshold of significance was set at $P \leq 0.05$.

2.3 Study 2: Evaluation of AT_1 receptor dependent superoxide production within the PVN

2.3.1 Drug treatment

Lewis (male *n*=3 and female *n*=3) and LPK (male *n*=3 and female *n*=3) rats were administered losartan (30 mg/kg/day; Cozavan, Alphapharm Pty Ltd, NSW, Australia) in the drinking water from age 4 to 12-14 weeks of age. Dosage was calculated every 2-4 days by measuring average daily water consumption and bodyweight of group caged animals (3 rats per cage). A separate cohort of male Lewis (*n*=3) and mixed sex LPK (male *n*=4 and female *n*=3) rats received plain tap water as a control.

2.3.2 Assessment of renal and cardiovascular function

Animals were acclimatised to metabolic cages routinely for one week prior to euthanasia. 48 h prior to euthanasia, animals were placed in metabolic cages to collect a 24 h urine sample and to measure 24 h water intake.

Blood pressure was measured consciously 48 h prior to euthanasia using tail-cuff plethysmography (IITC Inc. Life Science, Woodland Hills, CA, USA). Animals were acclimatised to the tail cuff procedure progressively for a week prior to data collection. Rats were restrained, placed in a heated (32°C) chamber and an externally controlled inflatable cuff was position at the base of the tail. A minimum of three measurements were made and the average value was used in the final analysis. Blood pressure was not recorded in *n*=1 untreated Lewis rat and *n*=1 untreated LPK rat.

At 12-14 weeks of age animals were deeply anaesthetised with 5% isoflurane (Baxter Healthcare Corporation, IL, USA) in 100% oxygen. Approximately 0.5 ml whole blood was collected via cardiac puncture and the animal was then euthanised by opening the thorax. Blood samples were centrifuged and stored at -80°C as per Study 1. Since the AT_1 receptor facilitates cardiac hypertrophy (Dahlof, 1995) and possibly renal cyst expansion (Keith et al., 1994), we dissected the heart and kidneys following death and measured whole heart weight, left ventricular weight and left kidney weight. Tissue weight parameters were not recorded in in *n*=1 untreated Lewis rat and *n*=1 untreated LPK rat.

Urine and plasma analysis was performed as per Study 1. Creatinine clearance was calculated with the following equation: $$\frac{\text{urinary creatinine (µmol/L)} \times \text{24 h urine volume (mL/min)}}{\text{plasma creatinine (µmol/L)}}$$

2.3.3 Detection of superoxide

Immediately following euthanasia, brains were removed, frozen in TissueTek® optimal cutting temperature compound (OCT) (ProSciTech, QLD, Australia) and stored at -80°C. In-situ ROS production was assessed with dihydroethidium (DHE), a cell-permeable chemical that readily reacts with superoxide (O_2^-) to form oxyethidium, a fluorescent compound that binds DNA (Cai et al., 2007). Fresh frozen 50 µm forebrain sections extending -1.3 to -2.3 mm from bregma were obtained using a cryostat (Leica CM1950, Leica Microsystems Pty Ltd.) and mounted

onto SuperFrost® Plus slides (Menzel-Glaser, Braunschweig, Germany). Sections were dried for 1 h at room temperature, rehydrated in PBS (5 min), incubated in DHE (1 μM; 5 min) in a dark chamber, washed in PBS, and then coverslipped with Dako fluorescent mounting medium (Dako Australia Pty Ltd., NSW, Australia). As a negative control, a subset of PVN sections (Lewis untreated *n*=2 and LPK untreated *n*=2) were preincubated in polyethylene glycol-superoxide dismutase (1000 U/ml), an enzyme that catalyses the conversion of superoxide to molecular oxygen or H_2O_2 (Noor et al., 2002), for 30 minutes at 37°C prior to DHE incubation. The majority of animals were processed in parallel as within strain untreated/treated pairs. Within 48 h of staining, DHE fluorescence was visualised with a confocal microscope (520 nm excitation and 600-620 nm emission; Leica TCS SP5, Leica Microsystems Pty Ltd.). Excitation and emission wavelengths were chosen so as to minimise the detection of non-specific H_2O_2 reaction products of DHE (Cai et al., 2007).

2.3.4 Superoxide quantification

DHE fluorescence was quantified with ImageJ software (National Institutes of Health, MD, USA) as previously described (Jensen, 2013). Briefly, RGB channels of the image were split and a threshold was applied to the red channel that permitted the visualisation of positively stained regions without background staining. To maximise the consistency of thresholding within and across animals, threshold range was set relative to a reference image in which positive and background staining had been pre-defined. Both sides of the PVN were outlined manually with reference to the rat brain atlas (Paxinos and Watson, 2013). Measurements were made of the percentage of positively stained area within the total area of the PVN. For each animal, both sides of the PVN were analysed from a total of 3-6 sections within -1.72 and -2.04 mm of bregma and averaged to provide a single value per animal for use in the final analysis. Data was then expressed relative to the average value for Lewis untreated controls.

2.3.5 Statistical analysis

All data are expressed as mean ± standard error of the mean (SEM). GraphPad Prism was used for statistical analysis. A two-way ANOVA with Bonferoni post-hoc test was used to detect differences between and within groups (strain and drug treatment). Lewis rats were precluded from statistical analysis for urinary protein parameters since urinary protein could only be detected in a single Lewis rat. Consequently we used a t test to detect differences in urinary protein and urinary protein: creatinine ratio in untreated and treated LPK rats. A threshold of significance was set at $P \leq 0.05$.

3. Results

3.1 Study 1: PVN microinjection and assessment of baroreflex function

3.1.1 Baseline characteristics

LPK rats had a lower body weight compared to Lewis controls and also exhibited greater plasma creatinine and plasma urea than Lewis rats (Table 1). Protein was detected in the urine of all LPK rats, but was not detected in Lewis rats.

Under urethane anaesthesia, LPK rats had elevated SBP and PP compared to Lewis rats (Table 2). However, MAP, DBP, HR and RSNA (μV) did not significantly differ between the strains.

Table 1. Bodyweight and renal function parameters in Lewis and Lewis Polycystic Kidney (LPK) rats.

	Lewis $_{(6)}$	LPK $_{(7)}$	*P*-value
BW (g)	360±7	260±6	<0.001
Urinary protein: creatinine ratio	0	4.05±0.92	-
Urinary protein (g/l)	0	0.74±0.16	-
Urinary creatinine (g/l)	0.97±0.14	0.19±0.01	<0.001
Plasma creatinine (µmol/l)	2.83±1.56	54.29±3.22	<0.001
Plasma urea (mmol/l)	9.27±0.61	32.36±1.56	<0.001

Values are expressed as mean ± SEM. *n* values per group are indicated by the subscript associated with each strain column. BW, bodyweight.

Table 2. Baseline blood pressure, heart rate and renal SNA in Lewis and Lewis Polycystic Kidney (LPK) rats.

	Lewis $_{(5)}$	LPK $_{(7)}$	*P*-value
MAP (mmHg)	85±6	94±5	0.278
SBP (mmHg)	127±8	177±10	0.006
DBP (mmHg)	65±7	63±4	0.827
PP (mmHg)	62±4	114±9	0.001
HR (bpm)	359±25	378±13	0.487
RSNA (µV)	4.6±2.5	6.1±1.9	0.331

Values are expressed as mean ± SEM. minimum *n* values per group are indicated by the subscript associated with each strain column. MAP, mean arterial pressure; SBP, systolic blood pressure; DBP, diastolic blood pressure; PP, pulse pressure; HR, heart rate; bpm, beats per minute; RSNA, renal SNA.

3.1.2 Anatomical location of microinjection sites

The anatomical location of microinjection sites is provided in Figure 3. The majority of injection sites were localised to the dorsal cap and posterior portion of the PVN between -1.8 and -2.04 mm of bregma. In a single Lewis rat, injection sites were located within the anterior PVN (-1.44 mm of bregma). The baseline response to kynurenic acid in this rat was not found to differ from Lewis rats where caudal portions of the PVN were targeted. In three animals (Lewis *n*=2 and LPK *n*=1), bilateral microinjection of kynurenic acid was histologically determined to lie outside of the PVN. These animals were assigned as anatomical controls.

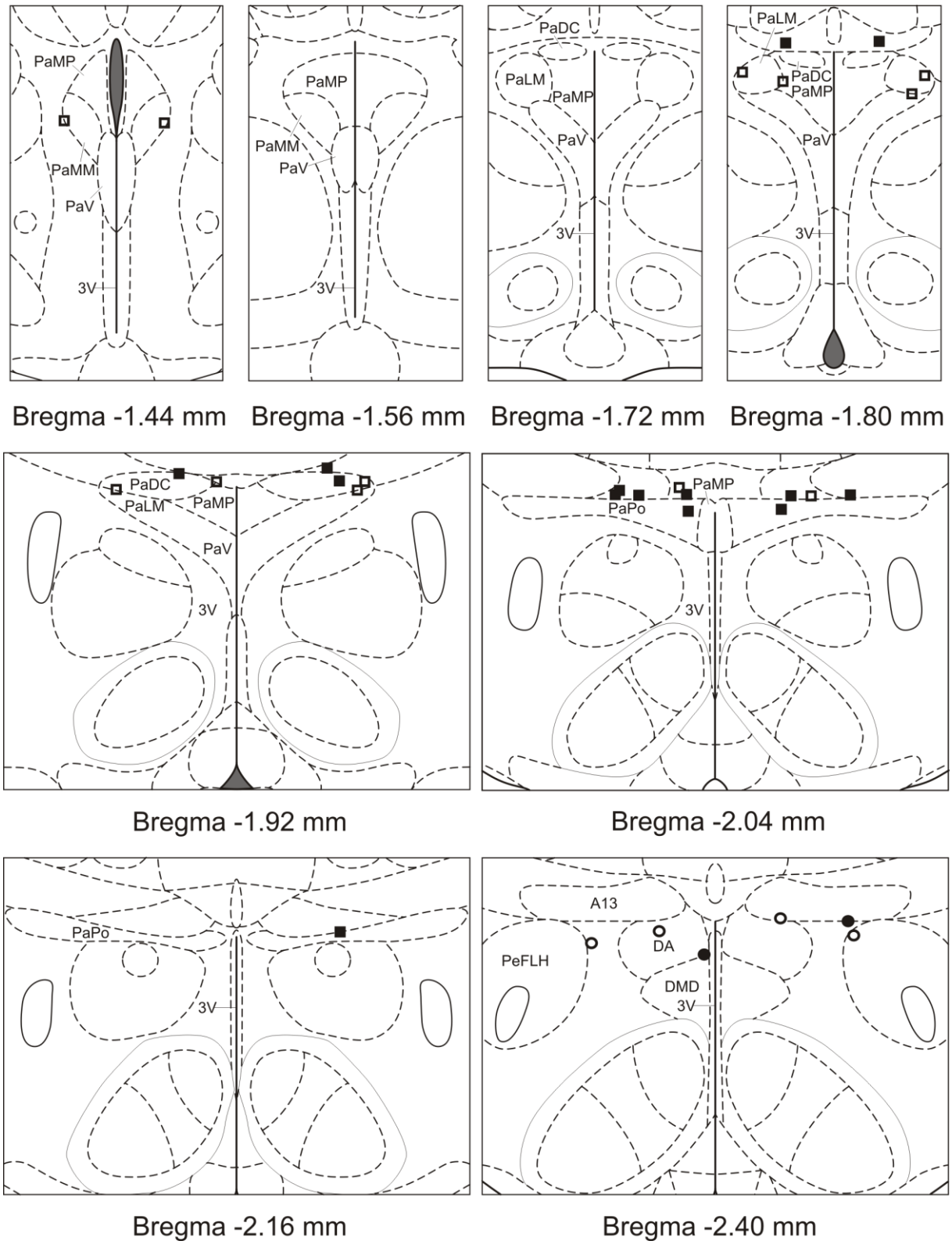

Figure 3: Anatomical diagrams illustrating the sites of PVN microinjections. Diagrams were modified from the rat brain atlas (Paxinos and Watson, 2013). Microinjection sites within the PVN are shown as open squares for Lewis rats (*n*=6) and filled squares for LPK rats (*n*=7). Microinjection sites outside of the PVN are shown as open circles for Lewis rats (*n*=2) and filled circles for LPK rats (*n*=1). PaMP, paraventricular nucleus medial parvocellular; 3V, third ventricle; PaMM, paraventricular nucleus medial magnocellular; PaV, paraventricular nucleus ventral part; PaDC, paraventricular nucleus dorsal cap; PaLM, paraventricular nucleus lateral

magnocellular; PaPo, paraventricular nucleus posterior part; PeFLH, perifornical lateral hypothalamus; A13, A13 cell group; DA, dorsal hypothalamic area; DMD, dorsomedial hypothalamic nucleus dorsal part.

3.1.3 The effect of bilateral PVN microinjection of kynurenic acid on arterial pressure, HR and RSNA

A representative trace illustrating the effect of bilateral microinjection of kynurenic acid into the PVN on arterial pressure, HR and RSNA in a Lewis and LPK rat is provided in Figure 4. In Lewis rats, microinjection of kynurenic acid into the PVN produced no significant change in MAP (85±6 vs. 81±7 mmHg $P>0.05$), SBP (127±8 vs. 117±9 mmHg $P>0.05$), DBP (65±7 vs. 58±6 mmHg $P>0.05$) or PP (62±4 vs. 59±9 mmHg $P>0.05$) over the 30 minute recording period. In contrast, microinjection of kynurenic acid reduced MAP (94±5 vs. 75±6 mmHg $P<0.0001$), SBP (177±9 vs. 145±10 mmHg $P<0.0001$), DBP (63±4 vs. 49±9 mmHg $P<0.0001$) and PP (114±9 vs. 96±9 mmHg $P<0.0001$) in LPK rats over the 30 minute recording period. In LPK, the reduction in SBP was evident by 5 minutes post microinjection ($P=0.05$; Figure 5A), reaching nadir by 15 minutes post microinjection ($P<0.0001$ 5 minutes vs. 15 minutes post microinjection) which was sustained throughout the 30 minute recording period ($P<0.0001$). Accordingly there was a significant strain effect in the SBP response, with the peak change in SBP greater in LPK compared to Lewis 15 to 30 minutes post microinjection ($P<0.0001$). Likewise, changes in MAP and PP at 30 minutes post microinjection were greater in LPK compared to Lewis rats ($P<0.05$). DBP however did not vary with strain (P=0.41). The depressor response in LPK rats was such that SBP was not significantly different to that seen in Lewis rats at 30 minutes post microinjection (145±10 mmHg vs. 117±9 mmHg; $P=0.23$).

Microinjection of kynurenic acid had no significant effect on HR in either strain over the 30 minute recording period ($P=0.17$; Figure 5B). RSNA did not vary with time in Lewis rats ($P=0.58$ baseline vs. 30 minute post microinjection; Figure 5C). In LPK, microinjection of kynurenic acid into the PVN produced a transient increase in RSNA at 5 minutes post microinjection ($P=0.03$; Figure 5C); however, no strain difference was noted at this time point ($P=0.97$). Both HR and RSNA responses were significantly more variable for Lewis compared to LPK animals. Grubb's tests did not identify any outliers.

The small number for offsite controls ($n=2$ Lewis and $n=1$ LPK) precluded their statistical analysis. Nevertheless, offsite kynurenic acid microinjection did not appear to change SBP in Lewis rats (126 vs. 121 mmHg and 144 vs. 132 mmHg; baseline vs. 30 minute post microinjection). In a single LPK, offsite kynurenic acid microinjection was associated with a reduction in SBP (191 vs. 155 mmHg; baseline vs. 30 minute post microinjection), that was comparable to LPK rats where kynurenic acid was microinjected within the PVN (-36 vs. -31±3 mmHg).

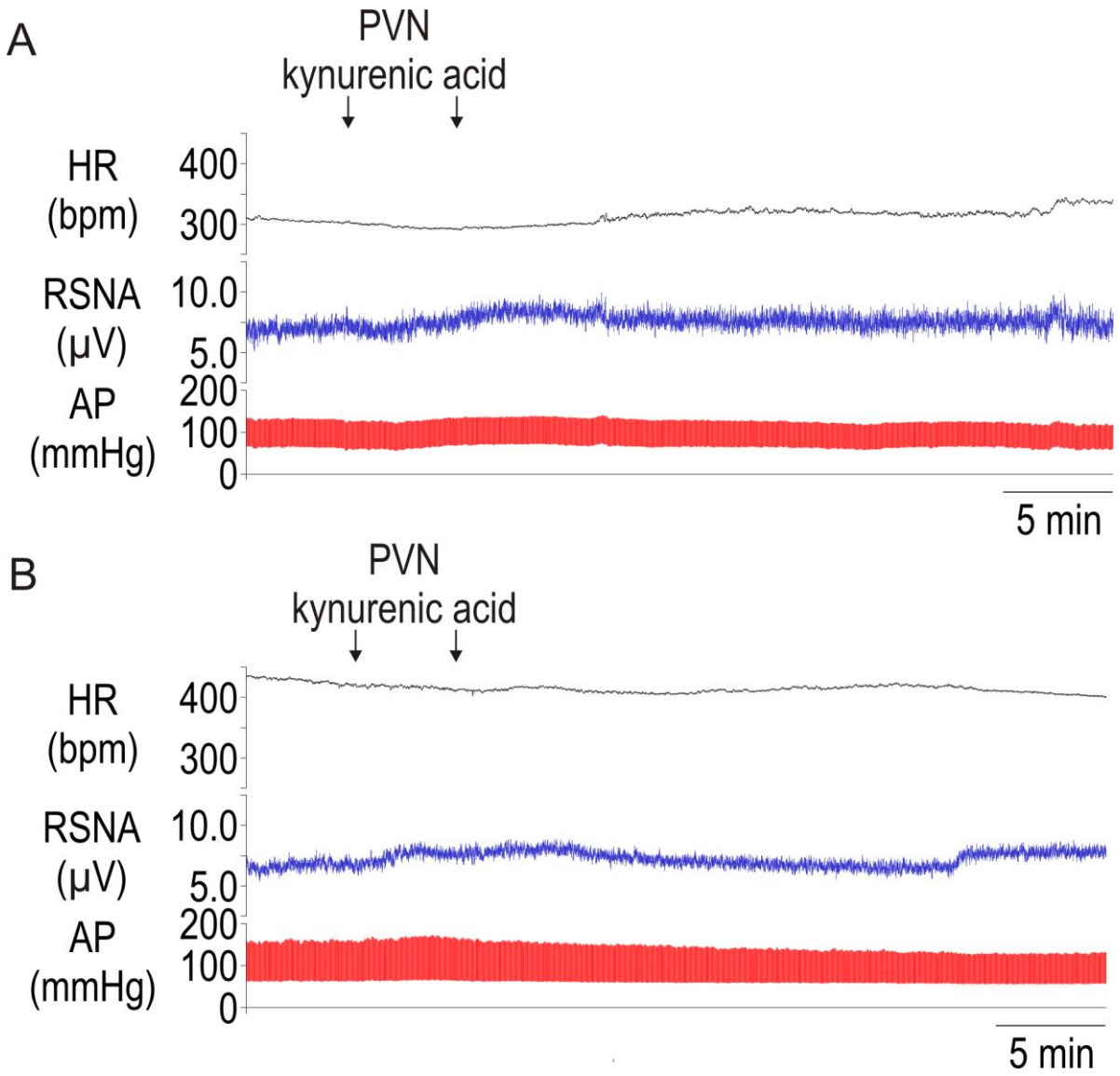

Figure 4: Representative traces illustrating the effects of bilateral microinjection of kynurenic acid (100 mM) into the paraventricular nucleus of the hypothalamus (PVN) on heart rate (HR), renal SNA (RSNA; raw and integrated (int RNSA)) and arterial pressure (AP) in **(A)** a Lewis and **(B)** a Lewis Polycystic Kidney (LPK) rat.

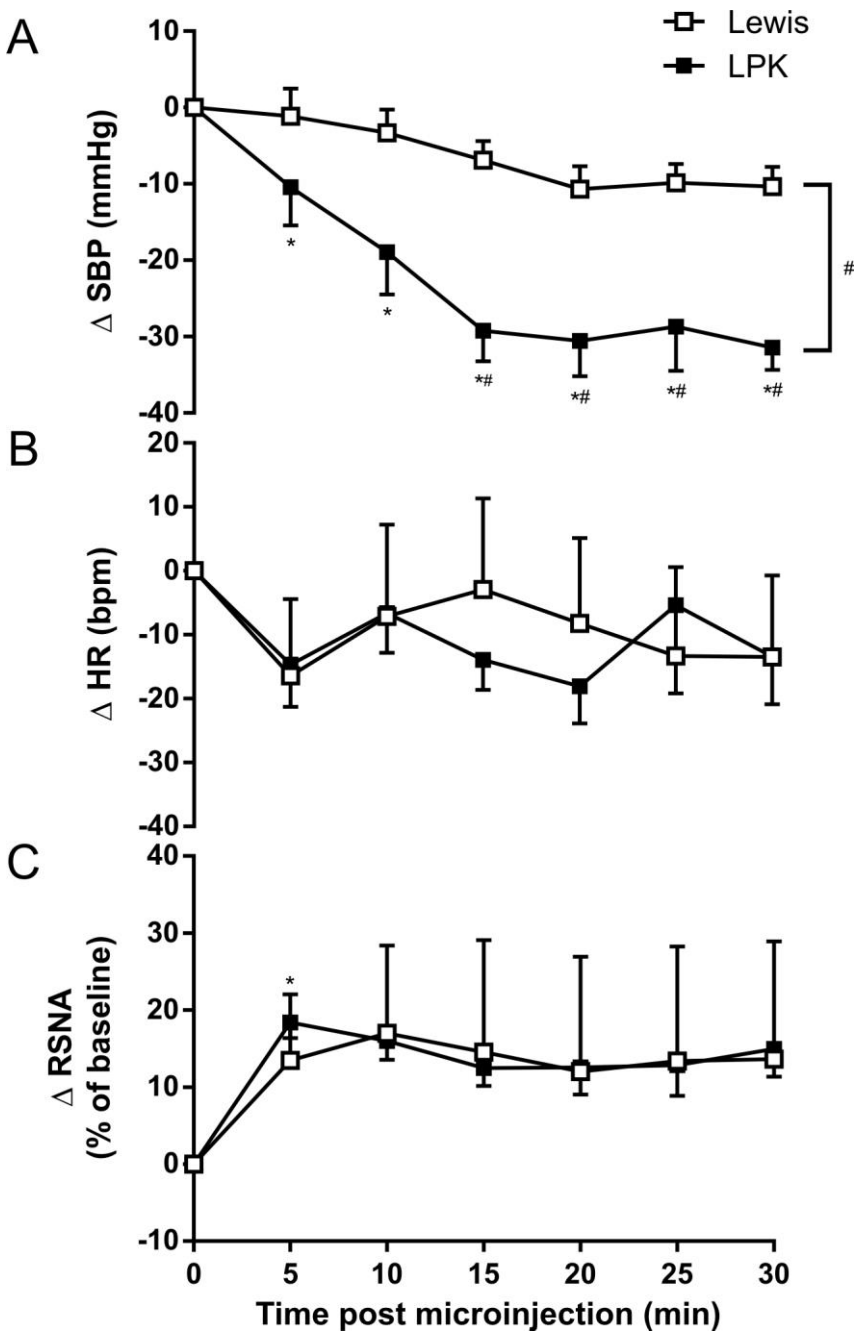

Figure 5: Grouped data showing the effect of bilateral microinjection of kynurenic acid (100 mM) into the paraventricular nucleus of the hypothalamus on **(A)** systolic blood pressure (SBP), **(B)** heart rate (HR) and **(C)** renal SNA (RSNA) in Lewis (*n*=5) and Lewis Polycystic Kidney (LPK; *n*=7) rats over a 30 minute post microinjection recording period. Data is presented as change from 5 minute baseline prior to microinjection. Values are expressed as mean ± SEM. * $P<0.05$ vs. baseline, # $P<0.05$ vs. Lewis rats at each time point and overall data sets as indicated. bpm, beats per minute.

3.1.4 Baroreflex control of HR and RSNA and the effect of bilateral PVN microinjection of kynurenic acid

Baroreflex function curves illustrating the relationship between SBP and HR or RSNA in Lewis and LPK before and after microinjection of kynurenic acid are illustrated in Figure 6.

Prior to microinjection of kynurenic acid, both HR and RSNA baroreflex function curves were shifted to the right in the LPK reflected by an increased SBP_{50} (Table 3). The SBP operating range of both HR and RSNA baroreflex function curves was greater in the LPK; however the HR and RSNA range was not different. Consistent with previous studies (Salman et al., 2014; Yao et al., 2015), the gain of both HR and RSNA baroreflex function curves was reduced in the LPK.

Despite producing a reduction in resting SBP, bilateral microinjection of kynurenic acid into the PVN did not affect SBP_{50} of either HR or RSNA baroreflex function curves and both curves remained shifted to the right in the LPK compared with Lewis following microinjection. Likewise, the SBP operating range remained increased for the HR baroreflex function curve and a trend toward remaining increased was noted for the RSNA baroreflex function curve (P=0.08). Microinjection of kynurenic acid into the PVN produced no improvement in the gain of either HR or RSNA baroreflex function curves in the LPK.

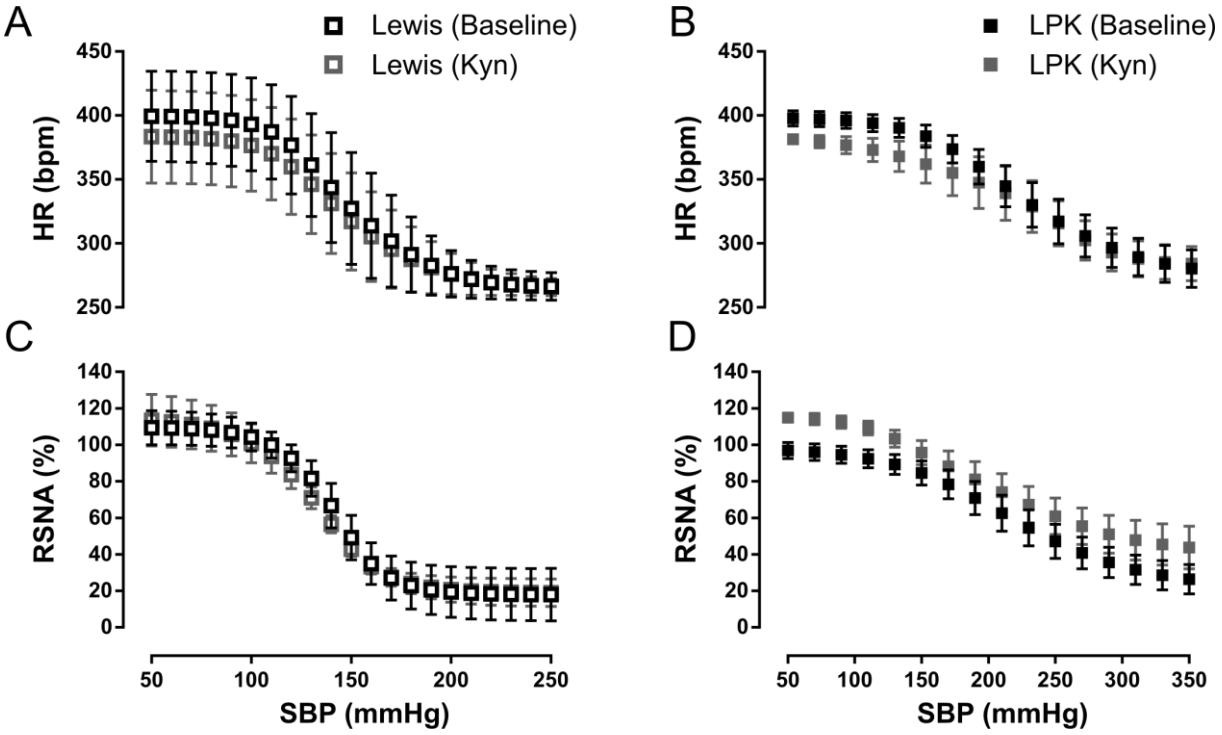

Figure 6: Grouped baroreflex function curves showing the effect of bilateral microinjection of kynurenic acid (100 mM) into the paraventricular nucleus of the hypothalamus (PVN) on the relationship between systolic blood pressure (SBP) and heart rate (HR) in **(A)** Lewis and **(B)** Lewis Polycystic Kidney (LPK) rats, and SBP and renal SNA (RSNA) in **(C)** Lewis and **(D)** LPK rats. Values are expressed as mean ± SEM. *n* values are detailed in Table 3. Kyn, kynurenic acid; bpm, beats per minute.

Table 3. Baroreflex parameters in Lewis and Lewis Polycystic Kidney (LPK) rats at baseline and following bilateral microinjection of kynurenic acid (100 mM) into the paraventricular nucleus of the hypothalamus.

Group	Lewis		LPK		*P*-value	
Parameter	Baseline	Kyn	Baseline	Kyn	Strain	Kyn
HR barocurve (*n*)	4		5			
SBP_{50} (mmHg)	146±10	143±10	223±17[a]	214±26[b]	0.017	0.611
SBP_{sat} (mmHg)	166±11	163±13	263±20[a]	251±22[b]	0.005	0.556
SBP_{thr} (mmHg)	125±9	124±8	184±16	177±30	0.070	0.711
SBP range (mmHg)	-19±21	-39±6	-79±13[a]	-74±11	0.011	0.588
Gain (bpm/mmHg)	-2.4±0.7	-1.9±0.3	-1.1±0.3	-1.0±0.2	0.048	0.318
Upper plateau (bpm)	400±35	384±36	399±6	385±3	0.996	0.272
Lower plateau (bpm)	266±10	265±5	274±16	283±13	0.440	0.602
Range (bpm)	134±31	119±32	125±16	102±13	0.653	0.240
RSNA barocurve (*n*)	4		7			
SBP_{50} (mmHg)	142±3	133±4	217±14[a]	198±19[b]	0.008	0.137
SBP_{sat} (mmHg)	158±3	153±1	269±18[a]	240±24[b]	0.004	0.182
SBP_{thr} (mmHg)	126±6	113±8	165±13	155±14	0.038	0.261
SBP range (mmHg)	-32±7	-40±9	-103±16[a]	-84±12	0.005	0.663
Gain (%/mmHg)	-1.9±0.1	-1.6±0.2	-0.5±0.1[a]	-0.6±0.1[b]	<0.001	0.347
Upper plateau (%)	110±10	115±15	99±5	116±3	0.555	0.126
Lower plateau (%)	18±14	19±8	21±8	41±12	0.429	0.139
Range (%)	92±17	96±20	77±8	75±10	0.341	0.867

Values are expressed as mean ± SEM. *n* indicates number of animals per group. [a] $P<0.05$ vs. Lewis rat at baseline, [b] $P<0.05$ vs. Lewis rat post microinjection. Kyn: kynurenic acid; HR, heart rate; bpm, beats per minute; SBP, systolic blood pressure; SBP_{50}, SBP at the midpoint of the curve; SBP_{sat}; SBP saturation; SBP_{thr}, SBP threshold; SBP range, SBP operational range; RSNA, renal SNA.

3.2 Study 2: Evaluation of AT_1 receptor dependent superoxide production within the PVN

3.2.1 Bodyweight and tissue weight

Bodyweight and tissue weight parameters are provided in Table 4. LPK rats had a lower bodyweight, greater left kidney weight and heart to body weight ratio than Lewis rats. Losartan treatment did not alter this. Left ventricular weight as a percentage of bodyweight showed both a strain and treatment effect and *post-hoc* analysis revealed that treatment reduced left ventricular weight as a proportion of bodyweight in LPK (P<0.01), but not in the in Lewis (P=0.31).

Table 4. Bodyweight and tissue weight parameters in Lewis and Lewis Polycystic Kidney (LPK) rats untreated and treated with losartan (30 mg/kg/day) from 4 to 12-14 weeks of age.

Group	Lewis		LPK		*P*-value	
Parameter	UnRx $_{(2)}$	LosRx $_{(6)}$	UnRx $_{(6)}$	LosRx $_{(6)}$	Strain	Rx
BW (g)	341±4	284±34	233±26	240±25	0.022	0.414
LKW (g)	1.3±0.1	1.2±0.2	10.7±1.4*	11.9±0.9$^{\#}$	<0.001	0.664
HW/BW	0.3±0.002	0.3±0.01	0.5±0.01*	0.5±0.02$^{\#}$	<0.001	0.190
LVW (% BW)	0.22±0.002	0.19±0.01	0.39±0.01*	0.34±0.01$^{\#\wedge}$	<0.001	<0.001

Values are expressed as mean ± SEM. minimum n values per group are indicated by the subscript associated with each strain and treatment column. * P<0.05 vs. untreated Lewis rat, # P<0.05 vs. losartan treated Lewis rat, ^P<0.05 vs. untreated strain-matched rat. UnRx, Untreated; LosRx, losartan treated; Rx, treated; BW, bodyweight; LKW, left kidney weight; HW, whole heart weight; LVW, left ventricular weight.

3.2.2 Blood pressure and renal parameters

Tail-cuff SBP and renal function parameters are provided in Table 5. Tail-cuff SBP was greater in LPK compared to Lewis rats, but there was no treatment effect. When compared to Lewis rats, LPK rats exhibited lower urinary creatinine as well as greater plasma creatinine, plasma urea, daily water consumption and daily urine production. Urinary protein was detected in all LPK rats, but was only detected in a single untreated Lewis rat. Creatinine clearance, an index of glomerular filtration rate (Rahn et al., 1999), was also reduced in LPK compared to Lewis rats. Treatment did not influence any renal function parameters in either strain (P>0.05).

Table 5. Tail-cuff blood pressure and renal function parameters in Lewis and Lewis Polycystic Kidney (LPK) rats untreated and treated with losartan (30 mg/kg/day) from 4 to 12-14 weeks of age.

Group	Lewis		LPK		*P*-value	
Parameter	UnRx (2)	LosRx (6)	UnRx (6)	LosRx (6)	Strain	Treatment
Tail-cuff SBP (mmHg)	113±2	110±2	209±8*	206±7#	<0.001	0.669
Urinary protein: creatinine ratio	0.4	0	3.8±0.9	5.6±1.5	-	0.312¥
Urinary protein (g/l)	0.1	0	0.8±0.2	1.1±0.2	-	0.321¥
Urinary creatinine (g/l)	1.4±0.1	1.1±0.1	0.2±0.02*	0.2±0.01#	<0.001	0.164
Creatinine clearance (ml/min)	2.6±0.5	2.5±0.2	0.6±0.1*	0.8±0.2#	<0.001	0.978
Plasma creatinine (µmol/l)	32.3±2.4	26.3±2.6	74.9±4.5*	87.9±14.8#	<0.001	0.712
Plasma urea (mmol/l)	6.6±0.2	6.9±0.2	26.1±1.6*	25.7±1.5#	<0.001	0.958
Daily water consumption/BW (ml)	0.06±0.003	0.09±0.01	0.24±0.02*	0.25±0.02#	<0.001	0.317
Daily urine production/BW (ml)	0.03±0.001	0.04±0.004	0.18±0.01*	0.18±0.01#	<0.001	0.828

Values are expressed as mean ± SEM. minimum *n* values per group are indicated by the subscript associated with each strain column. ¥ indicates t test for LPK rats. * $P<0.05$ vs. untreated Lewis rat, # $P<0.05$ vs. losartan treated Lewis rat. UnRx, Untreated; LosRx, losartan treated; SBP, systolic blood pressure; BW, bodyweight.

3.2.3 Superoxide production within the PVN and the effect of losartan treatment

Representative DHE stained PVN sections are shown in Figure 7A. Grouped DHE quantification data is provided in Figure 7B. Overall strain and treatment effects were detected for PVN DHE fluorescence. *Post-hoc* analysis revealed that PVN DHE fluorescence was greater in untreated LPK vs. Lewis (P=0.02), and that treatment did not change the levels in Lewis rats (P=0.53), but did reduce the levels in LPK rats (P=0.04) such that treated LPK rats were no longer different from untreated Lewis rats (P>0.05). The PVN DHE fluorescence was notably reduced in those sections pre-incubated with superoxide dismutase compared to sections without a pre-incubation period (Lewis untreated 0.29±0.01 vs. 1.0±0.2 and LPK untreated 0.17±0.03 vs. 2.0±0.3).

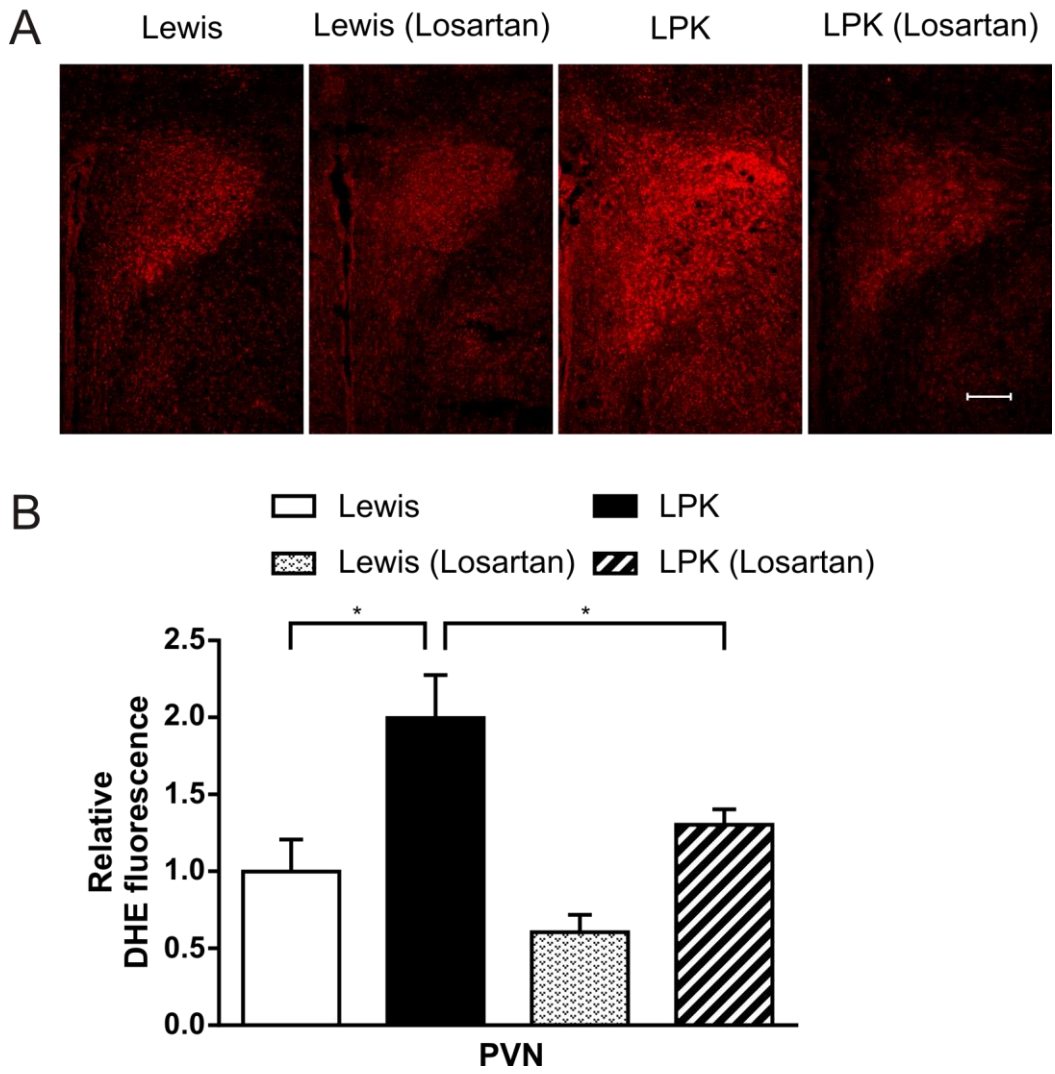

Figure 7: (A) Representative images of dihydroethidium (DHE) stained paraventricular nucleus of the hypothalamus (PVN) sections. Scale bar equal to 200 µm as indicated in the far right panel. **(B)** Grouped data showing quantification of DHE fluorescence within the PVN in Lewis and Lewis Polycystic Kidney (LPK) rats untreated (n=3 Lewis and n=7 LPK) and treated with losartan (n=6 Lewis and n=6 LPK; 30 mg/kg/day) from 4 to 12-14 weeks of age. Data are expressed relative to Lewis untreated control values. * P<0.05 between groups as indicated.

4. Discussion

The aim of this study was to determine whether glutamatergic inputs to the PVN contribute to hypertension and baroreflex dysfunction in the LPK model of CKD. We also sought to investigate whether ROS production is upregulated within the PVN in the LPK, and whether this is dependent upon the chronic activation of the Ang II AT_1 receptor. The major findings are that: (1) microinjection of the ionotropic glutamate receptor antagonist kynurenic acid into the PVN produced a greater depressor response in LPK rats compared to Lewis controls such that SBP was normalised; (2) blocking ionotropic glutamate receptors within the PVN was not associated with improved HR or RSNA baroreflex function in LPK rats; (3) superoxide is elevated within the PVN in LPK compared to Lewis rats, but is normalised by chronic treatment with the AT_1 receptor antagonist losartan. Collectively these findings indicate that enhanced glutamatergic activation of the PVN is important for the maintenance of hypertension, but not baroreflex dysfunction, in the LPK, and suggest that AT_1 receptor-dependent superoxide production is augmented within the PVN in this model of CKD. Our data highlight upregulated AT_1 receptor activity as a possible mechanism underlying the increase in glutamatergic tone of the PVN in CKD; although this remains to be tested.

4.1 LPK exhibit renal dysfunction and hypertension

Hypertension is an important complicating feature of CKD associated with poor cardiovascular and renal outcomes (Tozawa et al., 2003; Franklin and Wong, 2013). Here we confirm our previous findings that by 13 weeks of age LPK rats display the hallmarks of renal dysfunction, including impaired creatinine excretory function, uraemia and proteinuria, and that this occurs in conjunction with marked systolic hypertension (Phillips et al., 2007; Hildreth et al., 2013). In addition, the pulse pressure of LPK rats is significantly elevated, similar to humans with CKD, which likely reflects arterial stiffness (Ng et al., 2011b; Briet et al., 2012).

The genesis of hypertension in CKD is multifactorial. Certainly on the basis of the anti-hypertensive efficacy of diuretics and RAS blockers, plasma volume expansion and RAS activation are key contributing factors (Vasavada and Agarwal, 2003; Torres et al., 2014). However, approximately 20% of the CKD patient population exhibit treatment resistant hypertension (De Nicola et al., 2013), which is thought to be neurogenic in origin (Hering and Schlaich, 2015). In humans, there is direct evidence that renal deterioration is accompanied with elevated sympathetic outflow to muscle vascular beds (Klein et al., 2003a; Grassi et al., 2011), this being an important determinant of peripheral vascular resistance and therefore blood pressure (Vissing et al., 1989). Indeed, muscle SNA appears to positively predict hypertension in the PKD patient population (Klein et al., 2001). Recent studies reporting an anti-hypertensive effect of renal denervation in small uncontrolled CKD cohorts implies that augmented sympathetic outflow to the kidneys participates in the maintenance of hypertension in CKD (Hering et al., 2012; Kiuchi et al., 2013). However, the sympathetic nervous system does appear to be differentially activated in CKD, with evidence that cutaneous SNA is not elevated (Park et al., 2008; Grassi et al., 2009).

In contrast to our previous reports in conscious and anaesthetised rats (Salman et al., 2014; Salman et al., 2015b), we did not find that LPK rats exhibited increased RSNA at baseline relative to Lewis rats. However, our power to detect statistical differences in baseline RSNA was limited by the relatively low sample size for Lewis rats (n=5) as well as the large variability of recorded values, being more than two-fold greater than we have previously found in a similar anaesthetised preparation (Salman et al., 2014). Factors contributing to this variability may include the depth and duration of anaesthesia, artificial ventilation, the number fibres in the

nerve bundle, the amount of fluid at the electrode-nerve junction and the continuation of blood supply to the nerve (Burke et al., 2011).

4.2 Glutamatergic inputs to the PVN contribute to hypertension but not resting HR or RSNA in LPK

The PVN controls blood pressure through neural and humoral mechanisms

The PVN is a functionally heterogeneous collection of neurons that have the capacity to influence blood pressure through distinct neural and humoral faculties (Pyner, 2009). Parvocellular PVN pre-autonomic neurons are afforded control over central sympathetic outflow by virtue of projections that target the IML as well as pre-sympathetic neurons in the RVLM (Shafton et al., 1998). Trans-synaptic tracing studies have demonstrated that PVN pre-sympathetic neurons are anatomically primed to influence multiple sympathetic outflows, including renal, cardiac, lumbar, adrenal and splanchnic (Strack et al., 1989). There is also anatomical evidence that PVN pre-autonomic neurons target cardiac vagal preganglionic neurons located in their majority in the nucleus ambiguus and to a lesser extent the dorsal motor nucleus of the vagus (Buijs, 1978; Rinaman, 1998). Hence the PVN is in a pivotal position to coordinate autonomic control of the circulation.

In addition to the neural control of blood pressure, humoral faculties of the PVN may influence blood pressure through magnocellular neurons that secrete vasopressin and oxytocin into the peripheral circulation (Brown et al., 2013) and parvocellular corticotropin-releasing factor-synthesising neurons that regulate the downstream production of glucocorticoids at the adrenal gland (Benarroch, 2005). Among these PVN-regulated hormones, vasopressin, an anti-diuretic peptide and potent vasoconstrictor (Holmes et al., 2001), provides powerful control over arterial pressure, specifically in response to extracellular fluid hyperosmality and depletion (Schwartz and Reid, 1981; Thompson et al., 1986). This is in contrast to oxytocin, a peptide which may only contribute to vascular resistance when present in greater than normal physiological concentrations (Miller et al., 2002), and glucocorticoids, which act to enhance smooth muscle reactivity to vasoactive substances over extended time-scales (hours-days) through changes in gene expression (Ullian, 1999).

Differential control of arterial pressure by the PVN in Lewis and LPK

Under normal conditions PVN output activity contributes minimally, if at all, to the steady-state level of arterial pressure, HR and SNA, as indicated by a number of acute microinjection studies that have pharmacologically inhibited PVN efferent activity (Stocker et al., 2004; Li and Pan, 2007b; Martins-Pinge et al., 2012). Indeed this notion is supported by a recent study showing that long-term suppression of the PVN is without effect on blood pressure or HR in conscious normal rats (Geraldes et al., 2014). Here we show that acute inhibition of ionotropic glutamate receptors within PVN did not alter resting blood pressure, HR or RNSA in Lewis rats, which is consistent with previous reports in other healthy strains (Li et al., 2006) and with the current understanding concerning the functional organisation of ionotropic inputs within the PVN under normal conditions (Li et al., 2004; Li et al., 2006; Martins-Pinge et al., 2012). Afferent glutamatergic input to the PVN arises predominately from local interneurons as well as other hypothalamic and forebrain sites (Csaki et al., 2000; Ulrich-Lai et al., 2011). In addition, long ascending projections from the brainstem, although rarely glutamatergic themselves, are thought to recruit local glutamatergic interneurons (Affleck et al., 2012; Ziegler et al., 2012). It is thought that glutamatergic inputs to PVN pre-autonomic neurons are tonically active, although are offset by inhibitory GABAergic inputs such that the neurons are minimally

active at rest (Li et al., 2004; Li et al., 2006). Magnocellular vasopressin-secreting PVN neurons also receive tonic glutamatergic drive (Daftary et al., 1998); although is thought to be minimal during normal conditions since the concentration of circulating vasopressin is kept at a low level at rest and does not contribute to arterial pressure (Bussien et al., 1984). Hence in the Lewis it is likely that glutamatergic inputs to the PVN are sufficiently suppressed and therefore blockade of glutamate receptors had no effect on blood pressure, HR and RSNA. However given the large variability of HR and RSNA responses exhibited by Lewis animals, validating this point would benefit from a greater sample size.

However, in the LPK, blockade of ionotropic glutamate receptors within the PVN normalised SBP, supporting the notion that neurogenic contribution to blood pressure control by the PVN is central to the maintenance of hypertension in this model of CKD. This indicates that the organisation of ionotropic inputs within the PVN in LPK is altered, and could relate to either an enhancement of glutamate receptor activity or alternatively a reduction in ionotropic GABA receptor activity. Since we did not examine GABAergic control of the PVN in this study, we cannot distinguish between these two possibilities. Also, given the remarkable heterogeneity of PVN neurons that regulate blood pressure, we are unable to definitively determine the underlying cause of the depressor response following removal of glutamatergic inputs in LPK, as changes in cardiac output and sympathetic or vasopressin mediated changes in vascular resistance could all contribute.

Glutamatergic inputs to the PVN do not contribute to resting HR in LPK

It has been shown previously that glutamatergic activation of the PVN with NMDA evokes a tachycardic response that is dependent on both cardiac vagal and sympathetic efferents since this response is only abolished by simultaneous vagotomy and silencing of synaptic transmission within the IML (Kawabe et al., 2009). Furthermore, in-vitro evidence indicates that PVN efferents that project to cardiac vagal preganglionic neurons may differentially regulate cardiac vagal outflow depending on the region targeted within the medulla, with vasopressinergic terminals facilitating inhibitory control within the nucleus ambiguus (Wang et al., 2002) and oxytocinergic terminals facilitating excitatory drive within the dorsal motor nucleus of the vagus (Pinol et al., 2014). It is also possible that PVN efferents may regulate resting HR by modulating viscerosensory afferent transmission at the level of the NTS (Peters et al., 2008). Others have found that enhanced glutamatergic signalling within the PVN positively influences resting HR in rats with heart failure and essential hypertension, as silencing these inputs decreases HR in these animals (Li et al., 2003b; Li and Pan, 2007a). In comparison, our finding that HR did not change following removal of glutamatergic inputs to the PVN in LPK rats, suggests that these pathways are unlikely to contribute to resting HR in this model. A larger sample size would be necessary to substantiate this point.

Glutamatergic inputs to the PVN do not significantly contribute to resting RSNA in LPK

Contrary to our original hypothesis, we found that silencing glutamatergic signalling within the PVN in LPK was associated with an abrupt but transient increase in RSNA. It is possible that this initial renal sympathoexcitatory response in LPK was baroreflex mediated; although we consider this unlikely given the meagre reduction in SBP (10 mmHg) at this time point, which in light of our baroreflex data would not be expected to significantly elevate RSNA. Interestingly this short-acting excitatory RSNA response is in contrast to the sustained inhibitory lumbar SNA response we have previously found in LPK (Hildreth and Phillips, 2014), suggesting that glutamatergic inputs to PVN pre-sympathetic neurons are configured in a region-specific manner in the diseased state such that tonic glutamatergic drive inhibits renal,

but excites lumbar, sympathetic outflows. That the PVN has the capacity to differentially regulate SNA in response to robust physiological changes has been demonstrated previously, with evidence that inhibition of the PVN with the $GABA_A$ receptor agonist muscimol reduces lumbar SNA but is without effect on RSNA in rats chronically exposed to intermittent periods of hypoxia (Sharpe et al., 2013) or subjected to a 24 hour period of dehydration (Stocker et al., 2005). In contrast to the transient excitatory RSNA response exhibited in LPK rats, blocking glutamate signalling within the PVN in rats with heart failure produces a substantial reduction in RSNA concurrently with a decrease in arterial pressure (Li et al., 2003b). This indicates that the patterning of glutamatergic inputs to subpopulations of PVN neurons is differentially shaped during specific disease states. Additional studies will be required to determine whether enhanced glutamatergic drive contributes to splanchnic SNA in LPK since this is a regional sympathetic outflow that appears to be selectively upregulated in rats with Ang II-salt induced hypertension (Osborn and Fink, 2010).

Increased PVN-mediated peripheral secretion of vasopressin may contribute to hypertension in LPK

The inability of glutamatergic blockade within the PVN in LPK to reduce HR or RSNA suggests that the marked depressor response in this strain is mediated either by a reduction in sympathetic drive to other vascular beds or alternatively via a decrease in hormone activity at the vasculature (Figure 8). Preliminary data from our laboratory suggest that circulating vasopressin is greater in LPK compared to Lewis rats (Wise and Phillips, unpublished data). This is consistent with reports that plasma vasopressin is also elevated in rats with surgically reduced renal mass (Bouby et al., 1990) and in humans with PKD (Zittema et al., 2014). It is conceivable, therefore, that the reduction in blood pressure in LPK rats following microinjection of kynurenic acid into the PVN reflects decreased activity of vasopressin-secreting magnocellular PVN neurons. Indeed the slow onset of the depressor response in LPK rats is consistent with the half-life of circulating vasopressin (~15 min) (Czaczkes et al., 1964). However, additional studies are required substantiate this assertion. In that regard, isolating the PVN's humoral control of blood pressure with vagotomised and spinally-transected preparations would be valuable.

In contrast to the LPK, vasopressin-secreting magnocellular neurons are unlikely to play a significant role in the maintenance of hypertension enforced by glutamatergic drive of the PVN in the spontaneously hypertensive rat (SHR) model of essential hypertension (Li and Pan, 2007a) since neither acute nor chronic peripheral vasopressin antagonism effects blood pressure in this model (Sladek et al., 1987; Takeda et al., 1991). If we consider that plasma hyperosmolarity is the most powerful stimulus to evoke vasopressin secretion (Thompson et al., 1986) and that LPK rats (Phillips et al., 2007), and indeed humans with CKD (Zittema et al., 2014), have impaired urine concentrating ability, then it is tempting to speculate that enhanced glutamatergic drive of vasopressin-secreting magnocellular PVN neurons in LPK is an adaptation to the chronic challenge to plasma osmolality homeostasis imposed by the renal dysfunction. Consistent with this postulation is evidence that c-Fos expression is upregulated in the osmoreceptive circumventricular organ organum vasculosum laminae terminalis in LPK and other rat models of CKD (Ang et al., 2007; Palkovits et al., 2013). In addition to increased osmoreceptive input to the PVN, upregulated renal afferent nerve activity may provide an additional source of elevated excitatory drive to the PVN in LPK, as there is evidence that renal afferents increase their discharge from the diseased kidneys (Campese and Kogosov, 1995) and may excite magnocellular and pre-autonomic PVN neurons (Ciriello, 1998; Xu et al., 2015).

Offsite kynurenic acid microinjection also evokes a depressor response in LPK

Of note is our data showing that microinjection of kynurenic outside of the PVN in an LPK rat produced a comparable depressor response to those rats where kynurenic acid was microinjected within the PVN. It has been estimated that upon injection into neural tissue a 100 nl drug solution initially occupies a spherical area of extracellular space that has a radius of 484 µm (Nicholson, 1985; Gaede and Pilowsky, 2013). Thereafter the drug is expected to diffuse throughout the extracellular space, with its concentration decreasing as function of distance (Gaede and Pilowsky, 2013). Given that the epicentre of our offsite kynurenic acid microinjections in Lewis and LPK rats were located ~240 µm away from the caudal pole of the PVN, and that microinjection of kynurenic acid into the PVN at a concentration of as little as 3 mM has been reported to evoke a depressor response in SHR (Li and Pan, 2007a), it is conceivable that offsite kynurenic acid microinjection in these rats infiltrated an area of extracellular space that included a significant portion of the PVN neuronal population. Therefore, the principles of drug diffusion provide a plausible explanation for our data showing that microinjection of kynurenic acid within the immediate vicinity of the PVN reduced SBP in a single LPK rat.

4.3 Baroreflex dysfunction in LPK is independent of ionotropic glutamate receptor activity within the PVN

Centrally-mediated baroreflex dysfunction is an important pathological feature in CKD

Central processing of the baroreflex is particularly sensitive to environmental and physiological stimuli. Unique alterations in baroreflex function in response to exercise (Michelini and Stern, 2009), nociception (Pickering et al., 2003) and acute stress (Durocher et al., 2011) are examples of this. In the context of disease, the central nervous system may mediate maladaptive modifications in baroreflex function, with this being demonstrated in animal models of hypertension (Takeda et al., 1988; Salgado et al., 2007), heart failure (Patel et al., 2013), obesity (Huber and Schreihofer, 2010) and – as we have previously shown using the LPK – CKD (Salman et al., 2014). That LPK exhibit baroreflex dysfunction that is centrally-mediated is a pertinent finding since impaired cardiac baroreflex sensitivity inflates the risk of sudden cardiac death in individuals with CKD (Johansson et al., 2007; John et al., 2008), possibly by predisposing them to adverse arrhythmic events, as is the case in patients post-myocardial infarction (Farrell et al., 1991; Hohnloser et al., 1994).

Consistent with our previous reports (Hildreth et al., 2013; Salman et al., 2014; Yao et al., 2015), here we found that HR and RSNA baroreflex sensitivity (i.e. gain) is reduced in LPK compared to Lewis controls. This did, however, occur without a change in the range of HR or RSNA values recruited by the baroreflex. This is in contrast to our previous reports where we have found HR and RSNA range to be narrower in LPK rats of comparable age and renal function as the LPK used in the present study (Salman et al., 2014; Yao et al., 2015). It is possible that our ability to detect strain differences was limited due to the relatively small sample size for our baroreflex data. We also consider an important methodological difference, that being mechanical ventilation, which was consistently used in the current study but was only implemented previously as required (Salman et al., 2014). Activation of pulmonary stretch receptors by lung over-inflation has been shown to influence baroreflex function (Daly and Kirkman, 1989), and given that it is not known if this interaction is modified in renal disease, it is possible that mechanical ventilation contributed to these inconsistent findings. Nevertheless, that we did not find a strain difference in HR and RSNA range in the current study, but did identify that the baroreflex operated over a wider SBP range in the LPK, warrants an important consideration with respect to our baroreflex gain data. That is, since baroreflex gain represents the slope of the SBP-HR/RSNA relationship, then a widening of the operational

SBP range (x-axis) in LPK without a concurrent reduction in the HR/RSNA range (y-axis) would in and of itself support a reduction in the slope of the curve. Therefore the inherent interrelationship between these variables complicates the interpretation of our baseline gain data in the present study.

Glutamatergic drive of the PVN does not contribute to baroreflex dysfunction in LPK

A major aim of this study was to determine whether ionotropic glutamatergic inputs to the PVN contribute to impaired baroreflex control of HR and RSNA in LPK rats. A number of early studies showed that stimulating the PVN electrically (Ciriello and Calaresu, 1980b; Chen et al., 1996) or chemically with glutamate (Chen et al., 1996) or a glutamate analogue (Jin and Rockhold, 1989) blunts baroreflex evoked bradycardia, indicating that the PVN provides inhibitory control over baroreflex function and, importantly, that this may be driven by glutamate receptors. Inhibitory control of the baroreflex by the PVN may be mediated by projections to the NTS, where the majority of baro-activated neurons are inhibited upon stimulation of the PVN (Duan et al., 1999) and where vasopressin, a neuropeptide that is specific to PVN terminals in this region (Buijs, 1978; White et al., 1984), exerts an inhibitory action at the baroreceptor afferent-NTS neuron junction in-vitro (Bailey et al., 2006) and blunts baroreflex evoked bradycardia in-vivo (Michelini and Bonagamba, 1988; Kubo and Kihara, 1990). Furthermore, there are initial indications that the PVN may facilitate baroreflex dysfunction in SHR, with evidence that long-term suppression of the PVN partially restores spontaneous cardiac baroreflex sensitivity after 60 days (Geraldes et al., 2014); although it is possible that this improvement was peripherally-driven as hypertension was significantly attenuated in these rats.

Our results showing that glutamatergic blockade of the PVN does not alter HR or RSNA baroreflex function in LPK suggests that centrally-mediated baroreflex dysfunction in this CKD model is independent of glutamatergic inputs to the PVN. However, this does not preclude the possibility that glutamate-independent sources of excitatory inputs to the PVN contribute to baroreflex dysfunction in LPK. To this end, further investigations directed at silencing PVN output activity, for example with a $GABA_A$ agonist, are required. We also suggest that offsetting effects may have occurred as an indirect consequence of reducing PVN efferent activity. More specifically, if we consider that circulating vasopressin acts to enhance sympathetic baroreflex gain via the blood-brain barrier deficient area postrema (Cox et al., 1990), then decreased secretion of vasopressin following glutamatergic blockade of the PVN in LPK, which is strongly indicated although not directly ascertained here, may act in opposition to any potential improvement in baroreflex gain mediated by the removal of other PVN-dependent pathways.

Glutamatergic tone within the PVN does not contribute to baroreflex function in Lewis

Whether the PVN contributes to baroreflex function in the non-diseased state appears to be condition-dependent. In rats performing exercise, vasopressinergic PVN-NTS pathways are activated that serve to blunt reflex bradycardia and facilitate the co-occurrence of tachycardia with high blood pressure (Dufloth et al., 1997). In exercise-trained rats performing exercise, oxytocinergic PVN-NTS projections are co-activated and serve to increase HR baroreflex range and gain, thereby counteracting the actions of vasopressin and permitting the adaptive response of reduced exercise tachycardia (Braga et al., 2000; Higa et al., 2002). The presence of these functionally opposing condition-dependent neuronal subpopulations probably underlies the inconsistency of findings concerning the contribution of the PVN to baroreflex function in anaesthetised conditions. In that regard, it has been reported that crude lesions of the PVN in anaesthetised animals either increase (Ciriello and Calaresu, 1980b) or alternatively do not

influence (Patel and Schmid, 1988; Rockhold et al., 1990; Shih et al., 1995) baroreflex mediated bradycardia. Of these studies, only Patel and Schmid (1988) assessed the role of the PVN in the sympathetic baroreflex, finding that silencing neural activity within the PVN with lidocaine increased lumbar sympathetic baroreflex gain. In this study we found that administering kynurenic acid within the PVN did not alter baroreflex control of either HR or RSNA in Lewis rats, suggesting that tonic glutamatergic drive of the PVN does not contribute to baroreflex function in anaesthetised conditions in this strain. This finding is in contrast to another study in which baroreflex-mediated bradycardia was found to decrease following NMDA receptor antagonism of the PVN in conscious rats; however it important to note that trials were performed only 24 hour post-surgery in that study and as such the inadvertent recruitment of stress-related pathways cannot be ruled out (Crestani et al., 2010).

The baroreflex does not reset in LPK following removal of glutamatergic inputs to the PVN

Our data showing that HR and RSNA baroreflex function curves operate around a greater SBP set-point (i.e. the midpoint of the curve) in LPK relative to Lewis rats is consistent with that what has been reported in other hypertensive rats (Moyses et al., 1994) and humans (Grassi et al., 1998). Indeed, it is well established that a sustained deviation from the steady-state level of arterial pressure is associated with a chronic resetting of the operational set-point of the baroreflex in the direction of the pressure change. In a seminal study, McCubbin et al. (1956) demonstrated that chronic baroreflex resetting in hypertension is reflected in a shift in the discharge pattern of baroreceptor afferents. Using whole-fibre recordings of carotid and aortic baroreceptor afferent nerves, these authors showed that the arterial pressure values that were required to silence and saturate baroreceptor afferent discharge were greater in hypertensive dogs. Indeed, in agreement with this early report and subsequent studies in hypertensive rats (Sapru and Wang, 1976), we have previously shown that aortic depressor nerve responses are shifted to higher pressure values in LPK compared to Lewis rats (Salman et al., 2014).

Despite producing a large reduction in SBP in LPK rats, blocking glutamatergic inputs to the PVN failed to cause a resetting of the HR or RSNA baroreflex to lower pressure values. This indicates that either the duration of the depressor period in LPK was too short to enable peripheral resetting or that central processes are acting in opposition to prevent the entire baroreflex arc from resetting. Although baroreceptors partially reset within 15 minutes of a sustained change in arterial pressure (Undesser et al., 1984; Salgado and Krieger, 1988), this may only be 20-40% complete (Krieger, 1988). Hence the duration of the depressor response in LPK following glutamatergic blockade of the PVN may not have been sufficient to produce a detectable leftward shift in the baroreflex set-point. This result does, however, contrast our previous report where we found that bolus administration of losartan in LPK, which was associated with a comparable reduction in SBP to that exhibited by LPK here, was associated with leftward resetting of the RSNA baroreflex after 30 minutes (Yao et al., 2015). Although, rather than suggesting that a 30 minute depressor period is sufficient to cause peripheral resetting, instead this finding probably reflects the established role of central AT_1 receptors in mediating central baroreflex resetting (Head et al., 2002).

4.4 LPK exhibit elevated AT_1 receptor-dependent superoxide production within the PVN

Intracellular superoxide levels are elevated within the PVN in LPK

Cellular oxidative state is determined by the balance between ROS production and degradation. Oxidative signalling serves as an essential intermediate for a number of intracellular signalling cascades that regulate acute and chronic changes in neuronal activity (Massaad and Klann,

2011; Zimmerman, 2011). Increased brain ROS may play an important role in facilitating autonomic dysfunction in CKD. Using a salt-induced uninephrectomised rat model of CKD, Fujita et al. (2012) showed that acute central administration of the superoxide dismutase mimetic tempol decreased arterial pressure, HR and RSNA but was without effect in healthy rats. Consistent with this finding is our data showing that superoxide levels, assessed indirectly with DHE, are augmented within the PVN in LPK rats. However, we have previously found that chronic peripheral administration of tempol, which is blood-brain barrier permeable (Kwon et al., 2003), does not influence blood pressure in this model (Ding et al., 2012). This therefore implies that the heightened PVN oxidative state may not be obligatory for the development of hypertension in LPK. In order to test this assertion, however, further studies targeted at reducing PVN superoxide more selectively, for example with a vector that induces the overexpression of superoxide dismutase within the PVN (Zimmerman et al., 2002), will be required.

It has been reported previously that PVN superoxide levels are increased in other models of autonomic dysfunction, including in rodents with hypertension (Burmeister et al., 2011; Jancovski et al., 2013; Masson et al., 2014), heart failure (Guggilam et al., 2011) and diabetes (Patel et al., 2011). The two-fold change in DHE-detected superoxide levels within the PVN in LPK that we found here is similar to that reported in renovascular hypertensive mice (Burmeister et al., 2011) although less than the approximately three-fold increase reported in Ang II-infused mice (Masson et al., 2014) and diabetic rats (Patel et al., 2011). This difference may merely reflect experimental variation, although differences in disease characteristics (i.e. hyperglycaemia and high circulating Ang II) are also likely to have contributed.

Increased superoxide levels within the PVN in LPK is dependent on AT_1 receptor activity

Accumulating evidence has established the role of superoxide production as a secondary messenger of Ang II within the central nervous system. In a seminal study, Zimmerman et al. (2002) showed that central overexpression of superoxide dismutase substantially impairs the cardiovascular and behavioural effects of centrally-administered Ang II. It has since been demonstrated that upregulation of superoxide production by Ang II within the central nervous system is mediated by a G protein coupled process of the AT_1 receptor that stimulates nicotinamide adenine dinucleotide phosphate-oxidase (NADPH), a major enzymatic source of intracellular superoxide (Zimmerman et al., 2004; Infanger et al., 2006). Within the PVN, NADPH-dependent superoxide production is necessary to elicit the acute pressor and sympathoexcitatory actions of Ang II (Zhang et al., 2006). Using in-vitro whole-cell patch clamp recordings, Chen and Pan (2007) replicated this finding showing that Ang II-mediated excitation of pre-sympathetic PVN neurons is blocked in the presence of a superoxide scavenger.

We found that losartan treatment initiated early in the disease course was sufficient to restore PVN superoxide levels to non-disease levels in LPK, indicating that AT_1 receptors mediate superoxide production within the PVN and may be important to the chronic excitation of these neurons. The ability of losartan to normalise PVN superoxide levels was apparently independent of renal disease severity and blood pressure, as we found that indices of renal function and tail-cuff SBP measurements were not different between treatment groups at the single time point assessed. In contrast to the AT_1 receptor dependence of augmented PVN superoxide levels that we report in LPK here, Patel et al. (2011) found that losartan treatment did not significantly ameliorate high PVN superoxide in diabetic rats, which suggests that AT_1 receptor independent mechanisms, such as hyperglycaemia (Chappey et al., 1997), are responsible for the chronic oxidative state within the PVN in this model.

AT_1 receptor-dependent superoxide production within the PVN in LPK may be centrally or peripherally driven

Since we administered losartan peripherally in this study there are several possible ways in which chronic AT_1 receptor inhibition could reduce superoxide levels within the PVN in LPK. Considering that AT_1 receptors are distributed throughout the PVN (Lenkei et al., 1995), then if their activity is enhanced in LPK then direct blockade with losartan, which is blood-brain barrier permeable (Li et al., 1993), would blunt local superoxide production. This appears to the case in rats with heart failure since acutely administering losartan directly into the PVN reduces superoxide to control levels (Han et al., 2007). Clearly this mechanism infers that LPK either have augmented PVN extracellular Ang II concentration, AT_1 receptor density or intracellular coupling to NADPH. Certainly there is evidence that enhanced AT_1 receptor activity within the PVN in rats with renovascular hypertension (Chen et al., 2011a; Sun et al., 2012) and heart failure (Wang et al., 2005; Gan et al., 2014) could be due to both increased Ang II concentration as well as AT_1 receptor density. Further studies will be necessary to assess Ang II concentration and AT_1 receptor density within the PVN in LPK, and in this regard protein (e.g. western blot) and mRNA (e.g. reverse transcription-PCR) analyses will be valuable. During normal conditions circulating Ang II does not readily cross the blood-brain barrier (van Houten et al., 1980). Instead sites located outside of the blood-brain barrier such as the subfornical organ are responsible for relaying circulating Ang II information to central nuclei, such as the PVN, utilising Ang II as a neuropeptide (Lind et al., 1985; Anderson et al., 2001; Sakai et al., 2007). Interestingly, however, a recent report has shown that the permeability of the blood-brain barrier to Ang II is increased in hypertension (Biancardi et al., 2014), thereby raising the intriguing possibility that circulating Ang II may access the PVN, and indeed other autonomic nuclei, in hypertensive renal disease.

We also consider peripheral actions of AT_1 receptor blockade that could facilitate the downstream reduction in superoxide within the PVN in LPK. In rats with heart failure, myocardial ischemia resulting from the primary cardiac pathology activates cardiac sympathetic afferents which in turn stimulates superoxide production within the PVN via activation of the AT_1 receptor (Chen et al., 2015). Enhanced activity of this afferent pathway contributes to the sympathoexcitatory state in heart failure (Chen et al., 2015). Since we found that losartan treatment attenuated left-ventricular hypertrophy in LPK rats, consistent with the hypertrophic action of AT_1 receptors at the cardiomyocytes (Sadoshima and Izumo, 1993), then improved cardiac function in losartan treated LPK rats may have contributed to the reduction in superoxide levels within the PVN. Left-ventricular hypertrophy is also a characteristic of human CKD, and similarly responds to losartan treatment (Shibasaki et al., 2002). Accordingly, further studies are warranted to delineate the role of the cardiac sympathetic afferents in CKD. We envision that such experiments would take the form of testing the sympathetic response in Lewis and LPK rats to epicardial application of lidocaine and bradykinin to inhibit and active the cardiac sympathetic afferents, respectively (Zhu et al., 2002; Zhang et al., 2006).

4.5 Potential mechanisms by which the AT_1 receptor and superoxide may enhance glutamatergic tone within the PVN in LPK

Considering our data showing that AT_1 receptor-dependent superoxide production within the PVN is augmented in LPK, we consider possible mechanisms by which increased Ang II activity within the PVN may facilitate the enhancement of glutamatergic tone leading to hypertension in this CKD model (Figure 8). In-vitro patch clamp electrophysiology studies have demonstrated that the acute excitatory action of Ang II on PVN efferents is mediated indirectly by pre-synaptic inhibition of GABAergic inputs via the AT_1 receptor and the formation of

superoxide (Li et al., 2003a; Li and Pan, 2005; Chen and Pan, 2007). Therefore in LPK, Ang II-mediated reduction in GABAergic tone could enable glutamatergic drive to dominate. Further microinjection studies that acutely antagonise AT_1 receptors within the PVN will be valuable to test this postulation. Another pre-synaptic mechanism by which Ang II may potential upregulate glutamatergic activity within the PVN is by reducing glutamate reuptake. Glutamate reuptake is mediated by glutamate transporters that are located pre-synaptically, post-synaptically and extra-synaptically at the glia (Danbolt, 2001). In cultured astrocytes, AT_1 receptor activity negatively regulates glutamate transporter expression (Wu et al., 2010) and ROS decrease glutamate reuptake activity (Volterra et al., 1994). Indeed glutamate reuptake is blunted in hypothalamic astrocytes of rats with heart failure that also exhibit AT_1 receptor-dependent superoxide production (Han et al., 2007; Potapenko et al., 2012). In testing whether impaired astrocyte glutamate reuptake contributes to enhanced glutamatergic activity within the PVN in LPK, patch clamp electrophysiology experiments utilising the astrocyte-specific glutamate transporter inhibitor dihydrokainate would be valuable (Potapenko et al., 2012).

Accumulating evidence suggests that Ang II may also exert post-synaptic actions to facilitate an increase in glutamatergic activity by augmenting ionotropic glutamate receptor density and sensitivity. Glass et al. (2015) showed that chronic low dose Ang II treatment was associated with a substantial increase in NMDA receptor density at the dendritic surface within the PVN and that this was physiologically significant because selectively knocking down the obligatory NMDA receptor Glun1 subunit within the PVN largely prevented the formation of hypertension in this model. Consistent with this finding, Wang et al. (2013) showed using patch clamp electrophysiology that NMDA receptor currents were enhanced in PVN neurons from mice treated with low-dose Ang II, an effect that was blocked by bath application of a ROS scavenger. It would appear that superoxide formation represents a common intracellular messenger for the AT_1 and NMDA receptors since NADPH is also stimulated upon NMDA receptor activation (Brennan et al., 2009). It is well known that superoxide production is an essential secondary messenger for NMDA receptor-mediated long-term synaptic potentiation in hippocampal neurons (Klann, 1998; Huddleston et al., 2008). Within the PVN, NMDA receptor-induced ROS is enhanced by chronic AT_1 receptor activation which may be mediated by the mobilisation of cytoplasmic membrane NADPH close to NMDA receptors (Wang et al., 2013). Hence an upregulation of AT_1 receptor activity may facilitate NMDA receptor-mediated long-term synaptic potentiation both by enhancing NMDA receptor-induced superoxide production and by independently stimulating NADPH. Furthermore, AT_1 receptor- and NMDA receptor-induced ROS production may not only serve to enhance NMDA receptor activity, but may also increase AT_1 receptor activity, with evidence that superoxide positively regulates AT_1 receptor expression (Liu et al., 2008). Therefore we hypothesise that this cyclic, self-amplifying relationship between the AT_1 and NMDA receptors could act to augment glutamatergic tone within the PVN in LPK. We suggest that analyses of NMDA receptor expression and activity in-vitro in Lewis and LPK rats at baseline and following chronic losartan treatment or alternatively selective knockdown of the AT_1 receptor within the PVN (Chen et al., 2014) would be provide a means to this hypothesis.

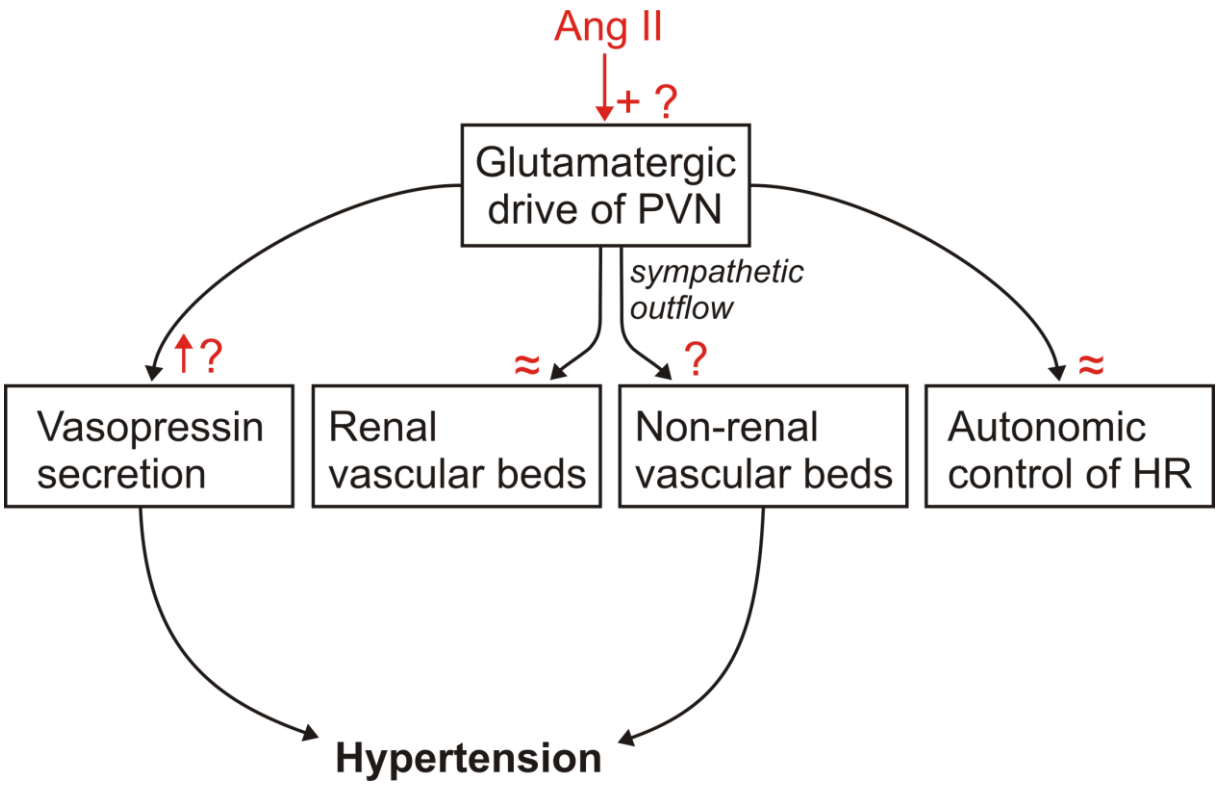

Figure 8: Diagram illustrating the proposed mechanism by which enhanced glutamatergic drive of the hypothalamic paraventricular nucleus (PVN) maintains hypertension in the Lewis Polycystic Kidney rat (LPK). Increased excitation of the PVN does not appear to significantly alter renal sympathetic outflow, nor does it influence resting heart rate (HR). Instead we speculate that increased glutamatergic tone of the PVN maintains hypertension in LPK by upregulating the secretion of vasopressin; although this remains to be tested. Similarly increased sympathetic outflow to non-renal vascular beds might contribute to the hypertension. In light of our data indicating that angiotensin II (Ang II) signalling within the PVN is augmented in LPK animals, we hypothesise that Ang II might be important in mediating the increase in glutamatergic drive of the PVN in this animal model of chronic kidney disease.

4.6 Methodological considerations and limitations

Brain microinjection

The brain microinjection technique is advantageous in that it permits focal drug delivery to pharmacologically manipulate discrete functional areas such as the PVN. However, drug diffusion is an inherent aspect of this method that must be considered when interpreting results. As previously mentioned, a 100 nl drug solution injected into neural tissue occupies an initial spherical area of extracellular space with a radius approximately equal to 484 µm (Nicholson, 1985; Gaede and Pilowsky, 2013). Thereafter the drug is expected to diffuse from the point-source throughout the extracellular space. However, since it is not possible to account for the non-linearity imposed by the various biophysical factors that influence the transport and availability of substances within the extracellular space (e.g. lipid solubility, molecular weight and degradation mechanisms), spatiotemporal drug diffusion is difficult to accurately model (Syková and Nicholson, 2008). Therefore, the inability to accurately determine the spatial extent of the affected neuronal population represents a limitation of the microinjection method. Considering the anatomical location of our PVN microinjection sites in the present study, it is possible that our results were influenced by drug diffusion to the dorsomedial hypothalamus

and anterior hypothalamic area – these being sites that have been implicated in cardiovascular regulation (Oparil et al., 1996; Queiroz et al., 2011). Additional offsite control injections targeting these regions will be beneficial in validating our data, as would further onsite PVN microinjections utilising smaller volumes and concentrations of kynurenic acid.

Additional work required for this study is the inclusion of vehicle microinjections. Others have previously used this control to demonstrate that responses are independent both of the vehicle solution and of injection-induced cell damage, thereby supporting drug specificity (Chen et al., 2011b; Streeter et al., 2011). Vehicle injections are particularly warranted in the current study since we co-injected fluorescent polystyrene microbeads with the drug solution in a subset of experiments. This method to mark injection sites with fluorescent microbeads at the time of the experimental microinjection was employed to validate the post-euthanasia labelling with pontamine sky blue dye. While fluorescent polystyrene microbeads afforded far superior anatomical labelling, it is possible that administering them to the PVN could have evoked an acute inflammatory response and consequently a change in neural activity. Although, we consider this unlikely given previous reports showing that vehicle solutions containing other polymer-based microbeads do not produce a discernible cardiovascular response upon microinjection into the PVN (Chen et al., 2011b; Streeter et al., 2011). Indeed we observed that responses were comparable in those animals that received kynurenic acid PVN microinjections with and without fluorescent microbeads.

Translational considerations

As a model of CKD that develops renal dysfunction progressively akin to the human disease (Phillips et al., 2007), the LPK is particularly advantageous over models of sudden onset surgically or chemically induced renal dysfunction. Although unlike the human disease which affects both sexes, we have restricted our microinjection study to male rats here. This is an important consideration because the female form of CKD is generally less severe and may differentially respond to treatments both in LPK and humans (Phillips et al., 2007; Carrero, 2010; Jeewandara et al., 2015). While we have previously shown that centrally-mediated baroreflex dysfunction is also present in female LPK (Salman et al., 2015a), it is possible that the underlying neural circuitry differs from male LPK due to the action of female sex hormones at key autonomic nuclei (Saleh and Connell, 2000). Consequently further investigations in both sexes will be necessary to understand the pathogenesis of baroreflex dysfunction in CKD.

As well as the sex-bias of our microinjection study, the use of anaesthesia poses an experimental caveat also worthy of consideration. We used an anaesthetised preparation here since chronic recording of sympathetic nerve activity in conscious rats is currently not technically feasible. Furthermore, the chronic catheterisation required to administer intravenous drugs and perform microinjections in conscious animals is highly invasive and could therefore independently influence cardiovascular and autonomic function. We used urethane anaesthesia here since compared to other anaesthetics (e.g. inhalation, barbiturate and dissociative) it has minimal effects on cardiorespiratory function and provides stable long-term anaesthesia (Tremoleda et al., 2012). Nevertheless, it has been reported, rather inconsistently, that urethane increases, decreases or alternatively produces no change in blood pressure, HR and RSNA in rats (Shimokawa et al., 1998; Holobotovskyy et al., 2004; Wang et al., 2014). Urethane might affect these parameters by way of influencing neurotransmission within the NTS (Accorsi-Mendonca et al., 2007). We found that when compared to SBP measured consciously with tail-cuff plethysmography, SBP measured intra-arterially under urethane anaesthesia was markedly less in LPK but slightly greater in Lewis, thereby indicating that these strains may differ in their sensitivity to urethane. Also of relevance to our results is evidence that urethane increases

plasma vasopressin levels (Faber, 1989), which conceivably would have exaggerated the depressor response that we report in LPK following glutamatergic blockade of the PVN if the mechanism was mediated by circulating vasopressin as we have hypothesised. Hence cardiovascular and autonomic function under urethane anaesthesia must be considered with these caveats.

Assessment of autonomic function

Given the pathological importance of the sympathetic nervous system in disease, it highly valuable to be able to compare levels of regional SNA between animals. Here we have compared whole-fibre RSNA between strains by quantifying integrated SNA voltage – a measure that incorporates both the frequency and amplitude of the raw SNA signal. This approach has been questioned because the amplitude component of the SNA signal is dependent on a number factors that may undeterminably vary between animals, such as the number of fibres in the nerve bundle, the amount of moisture at the nerve-electrode junction and the continuation of blood supply to nerve (Burke et al., 2011). However, between-animal SNA voltage comparisons have been used previously to provide valuable information concerning regional sympathoexcitation in SHR (Judy et al., 1976). As an alternative measure of regional SNA, the burst frequency of whole-fibres has been used previously (Nishi et al., 2010). However, this measurement does not provide insight into the amount of sympathetic fibres recruited and is therefore an incomplete description of central sympathetic outflow (Burke et al., 2011). Nevertheless, concerns regarding the comparison of voltage values of SNA can be alleviated when evaluating within-animal SNA responses by scaling SNA to a baseline (100%) and death (0%) value, as we have done here.

In the present study we used HR as an indirect measure of cardiac autonomic outflow since it is technically challenging to isolate cardiac vagal and sympathetic branches for recording in-vivo. This measure does, however, neglect that alterations at the pre- or post-ganglionic junction impair the ability of the heart to respond to a change in central autonomic outflow. While we have previously shown that left vagal stimulation produces comparable HR responses in Lewis and LPK (Salman, 2014; Salman et al., 2015a), suggesting intact peripheral parasympathetic efferent function, it has not been tested whether peripheral cardiac sympathetic efferent function is altered in LPK. An additional limitation of using HR as an indicator of cardiac autonomic outflow is the inability to discriminate between the individual roles of vagal and sympathetic efferents. This therefore limits the interpretation of our finding that HR did not change following glutamate blockade of the PVN because it is possible that a counteracting change in vagal and cardiac sympathetic outflows occurred rather than no change. However with respect to baroreflex-mediated HR responses, previous studies have clearly demonstrated that the cardiac vagus predominately mediates both reflex bradycardia and tachycardia (Parlow et al., 1995) whereas cardiac sympathetic efferents only contribute partially to reflex tachycardia (Chen et al., 1982). Therefore, the assessment of HR baroreflex function in this study most likely reflects the predominant action of cardiac vagal rather than cardiac sympathetic efferents.

Assessment of baroreflex function with induced changes in blood pressure is dependent on the function of the peripheral baroreceptors. Consequently indirect changes within the periphery following manipulation of the PVN could have altered baroreceptor transduction and therefore the overall function of the baroreflex arc. While acute reductions in arterial pressure exhibited in LPK following glutamatergic blockade of the PVN is almost certainly not sufficient to induce vascular structural changes, changes in circulating hormones could conceivably alter baroreceptor transduction. Indeed, circulating vasopressin has been shown to sensitise aortic baroreceptor afferents (Abboud et al., 1986). Therefore, further investigations of centrally-

mediated baroreflex dysfunction in LPK will benefit from direct aortic depressor nerve stimulation (Salman et al., 2014).

Tail-cuff plethysmography

We employed tail-cuff plethysmography to assess blood pressure at a single time-point in our losartan treatment study. This method affords non-invasive conscious recordings of blood pressure that have been shown to correlate well with readings obtained by invasive intra-arterial approaches (Bunag, 1973; Ibrahim et al., 2006). However, the inherent short-term variability of blood pressure is known to be inflated by a number of factors associated with the tail-cuff procedure, including restraint-associated stress, heating of the tail and positioning of the cuff (Ibrahim et al., 2006). In this study, animals were routinely handled and acclimatised to the tail-cuff procedure in the week prior to data collection, however we concur that one week may not have been adequate to sufficiently minimise restraint-stress. In that regard, multiple weekly measurements over the treatment period would have assisted in further minimising restraint-stress, while also providing the additional benefit of being able to track blood pressure over time. As an alternative method to assess blood pressure consciously, intra-arterial radiotelemetry affords long-term ambulatory average blood pressure measurements and will be utilised for future studies.

We conceive that the degree of unreliability associated with acutely measuring blood pressure with tail-cuff plethysmography could have underscored the absence of a blood pressure response following losartan treatment in LPK because previously we have shown that the development of hypertension in this model is greatly impaired by chronic inhibition of Ang II production (Ng et al., 2011a) or AT_1 receptor blockade with an analogous drug (Ameer and Phillips, unpublished data). However, we also consider the alternative possibility that rats received a non-depressor dose of losartan. While the dose administered in the drinking water here is greater than that previously reported to have an anti-hypertensive effect in other strains (Morton et al., 1992; Patel et al., 2011), we found that losartan had poor water solubility. Hence we are unable to determine whether the apparent absence of an anti-hypertensive effect in LPK is due to invalid recordings of blood pressure or because rats received a non-depressor dose of losartan. Further studies will benefit from administering losartan through other routes (e.g. oral gavage, subcutaneous osmotic minipump or with food).

Superoxide quantification

Due to its unstable nature and low intracellular concentration, measurement of superoxide is largely restricted to indirect methods (de Campos et al., 2015). The redox-sensitive fluorophore DHE has been extensively used to detect superoxide in isolated tissues and cells (Pannirselvam et al., 2005; Patel et al., 2011; Shen et al., 2015). The reaction products of DHE can be quantified in-situ with image analysis or in cell extracts with high performance liquid chromatography (HPLC) (Cai et al., 2007). In-situ quantification of DHE fluorescence affords greater spatial resolution than the HPLC method in that regional differences can be detected (e.g. subnuclei of the PVN), although its accuracy is highly dependent upon factors governing fluorescence intensity. Within an image, the intensity of a pixel is dependent on the number of fluorophores present at the corresponding area of the specimen – which is intimately reliant on the staining procedure – as well as the image acquisition parameters (e.g. excitation/emission spectra, focus, gain and pinhole settings) (Waters, 2009). Although we were stringent in ensuring consistent staining and imaging procedures across samples, natural variability is expected which could limit the accuracy of this method. Furthermore, oxidation of DHE with H_2O_2 yields fluorescent products with an excitation/emission spectra that partially overlaps with

superoxide-specific DHE products (Cai et al., 2007). In that regard, the HPLC method provides greater sensitivity in quantifying superoxide since it is possible to distinguish H_2O_2- and superoxide-specific DHE products (Kalyanaraman et al., 2014). Therfore the HPLC based method of DHE quantification on micropunch dissected sections from the PVN will be a useful approach to confirm the results of the present study.

5. Conclusion

Hypertension and baroreflex dysfunction contribute to the disproportionality high incidence of cardiovascular mortality in CKD (Johansson et al., 2007; Franklin and Wong, 2013). In the present study we tested the hypothesis that excitatory glutamatergic drive of the PVN contributes to hypertension and impaired baroreflex control of HR and RSNA in the LPK model of CKD. Our results suggest that enhanced glutamatergic tone within the PVN is essential for the maintenance of hypertension, but not baroreflex dysfunction, in the LPK rat. Hence the pathogenesis of centrally-mediated baroreflex dysfunction in this CKD model remains to be determined. We provide a mechanistic insight into the upregulation of neuronal activity within the PVN in LPK, showing that LPK have elevated superoxide levels within the PVN that is dependent on chronic AT_1 receptor activity. While further studies will be required to determine whether the heightened oxidative state within the PVN in the LPK contributes to altered cardiovascular and autonomic control, this finding nevertheless reinforces the therapeutic importance of AT_1 receptor blockers in CKD.

6. References

Abboud, F.M., Aylward, P.E., Floras, J.S., and Gupta, B.N. (1986). Sensitization of aortic and cardiac baroreceptors by arginine vasopressin in mammals. *J. Physiol.* 377**,** 251-265.

Accorsi-Mendonca, D., Leao, R.M., Aguiar, J.F., Varanda, W.A., and Machado, B.H. (2007). Urethane inhibits the GABAergic neurotransmission in the nucleus of the solitary tract of rat brain stem slices. *Am. J. Physiol. Regul. Integr. Comp. Physiol.* 292**,** R396-402.

Affleck, V.S., Coote, J.H., and Pyner, S. (2012). The projection and synaptic organization of NTS afferent connections with presympathetic neurons, GABA and nNOS neurons in the paraventricular nucleus of the hypothalamus. *Neuroscience* 219**,** 48-61.

Agarwal, A., Anand, I.S., Sakhuja, V., and Chugh, K.S. (1991). Effect of dialysis and renal transplantation on autonomic dysfunction in chronic renal failure. *Kidney Int.* 40**,** 489-495.

Agarwal, S.K., Gelsema, A.J., and Calaresu, F.R. (1990). Inhibition of rostral VLM by baroreceptor activation is relayed through caudal VLM. *Am. J. Physiol.* 258**,** R1271-1278.

Anderson, J.W., Smith, P.M., and Ferguson, A.V. (2001). Subfornical organ neurons projecting to paraventricular nucleus: whole-cell properties. *Brain Res.* 921**,** 78-85.

Ang, S.A., Harrison, J.L., Powers-Martin, K., Reddrop, C., Mckitrick, D.J., et al. (2007). "c-Fos activation in renal hypertension", in: *Proceedings of the High Blood Pressure Research Council of Australia 2006 Annual Scientific Meeting*: Hypertension, 1462-1481.

Antunes, V.R., Yao, S.T., Pickering, A.E., Murphy, D., and Paton, J.F. (2006). A spinal vasopressinergic mechanism mediates hyperosmolality-induced sympathoexcitation. *J. Physiol.* 576**,** 569-583.

Aviado, D.M., and Schmidt, C.F. (1955). Reflexes from stretch receptors in blood vessels, heart and lungs. *Physiol. Rev.* 35**,** 247-300.

Bailey, T.W., Jin, Y.H., Doyle, M.W., Smith, S.M., and Andresen, M.C. (2006). Vasopressin inhibits glutamate release via two distinct modes in the brainstem. *J. Neurosci.* 26**,** 6131-6142.

Balamuthusamy, S., Srinivasan, L., Verma, M., Adigopula, S., Jalandhara, N., et al. (2008). Renin angiotensin system blockade and cardiovascular outcomes in patients with chronic kidney disease and proteinuria: a meta-analysis. *Am. Heart J.* 155**,** 791-805.

Bavanandan, S., Ajayi, S., Fentum, B., Paul, S.K., Carr, S.J., et al. (2005). Cardiac baroreceptor sensitivity: a prognostic marker in predialysis chronic kidney disease patients. *Kidney Int.* 67**,** 1019-1027.

Benarroch, E.E. (2005). Paraventricular nucleus, stress response, and cardiovascular disease. *Clin. Auton. Res.* 15**,** 254-263.

Biancardi, V.C., Son, S.J., Ahmadi, S., Filosa, J.A., and Stern, J.E. (2014). Circulating angiotensin II gains access to the hypothalamus and brain stem during hypertension via breakdown of the blood-brain barrier. *Hypertension* 63**,** 572-579.

Blessing, W.W. (1988). Depressor neurons in rabbit caudal medulla act via GABA receptors in rostral medulla. *Am. J. Physiol.* 254**,** H686-692.

Blinder, K.J., Gatti, P.J., Johnson, T.A., Lauenstein, J.-M., Coleman, W.P., et al. (1998). Ultrastructural circuitry of cardiorespiratory reflexes: there is a monosynaptic path between the nucleus of the solitary tract and vagal preganglionic motoneurons controlling atrioventricular conduction in the cat. *Brain Res.* 785**,** 143-157.

Bouby, N., Bachmann, S., Bichet, D., and Bankir, L. (1990). Effect of water intake on the progression of chronic renal failure in the 5/6 nephrectomized rat. *Am. J. Physiol.* 258**,** F973-979.

Brack, K.E., Coote, J.H., and Ng, G.A. (2004). Interaction between direct sympathetic and vagus nerve stimulation on heart rate in the isolated rabbit heart. *Exp. Physiol.* 89**,** 128-139.

Braga, D.C., Mori, E., Higa, K.T., Morris, M., and Michelini, L.C. (2000). Central oxytocin modulates exercise-induced tachycardia. *Am. J. Physiol. Regul. Integr. Comp. Physiol.* 278**,** R1474-R1482.

Brennan, A.M., Suh, S.W., Won, S.J., Narasimhan, P., Kauppinen, T.M., et al. (2009). NADPH oxidase is the primary source of superoxide induced by NMDA receptor activation. *Nat. Neurosci.* 12**,** 857-863.

Briet, M., Boutouyrie, P., Laurent, S., and London, G.M. (2012). Arterial stiffness and pulse pressure in CKD and ESRD. *Kidney Int.* 82**,** 388-400.

Brown, C.H., Bains, J.S., Ludwig, M., and Stern, J.E. (2013). Physiological regulation of magnocellular neurosecretory cell activity: integration of intrinsic, local and afferent mechanisms. *J. Neuroendocrinol.* 25**,** 678-710.

Buijs, R.M. (1978). Intra- and extrahypothalamic vasopressin and oxytocin pathways in the rat. Pathways to the limbic system, medulla oblongata and spinal cord. *Cell Tissue Res.* 192**,** 423-435.

Bunag, R.D. (1973). Validation in awake rats of a tail-cuff method for measuring systolic pressure. *J. Appl. Physiol.* 34**,** 279-282.

Burke, S.L., Lambert, E., and Head, G.A. (2011). New approaches to quantifying sympathetic nerve activity. *Curr. Hypertens. Rep.* 13**,** 249-257.

Burmeister, M.A., Young, C.N., Braga, V.A., Butler, S.D., Sharma, R.V., et al. (2011). In vivo bioluminescence imaging reveals redox-regulated activator protein-1 activation in paraventricular nucleus of mice with renovascular hypertension. *Hypertension* 57**,** 289-297.

Bussien, J.P., Waeber, B., Nussberger, J., Schaller, M.D., Gavras, H., et al. (1984). Does vasopressin sustain blood pressure of normally hydrated healthy volunteers? *Am. J. Physiol.* 246**,** H143-147.

Cai, H., Dikalov, S., Griendling, K.K., and Harrison, D.G. (2007). Detection of reactive oxygen species and nitric oxide in vascular cells and tissues: comparison of sensitivity and specificity. *Methods Mol. Med.* 139**,** 293-311.

Campese, V.M., and Kogosov, E. (1995). Renal afferent denervation prevents hypertension in rats with chronic renal failure. *Hypertension* 25**,** 878-882.

Carrero, J.J. (2010). Gender differences in chronic kidney disease: underpinnings and therapeutic implications. *Kidney Blood Press. Res.* 33**,** 383-392.

Cassaglia, P.A., Shi, Z., Li, B., Reis, W.L., Clute-Reinig, N.M., et al. (2014). Neuropeptide Y acts in the paraventricular nucleus to suppress sympathetic nerve activity and its baroreflex regulation. *J. Physiol.* 592**,** 1655-1675.

Chandra, P., Sands, R.L., Gillespie, B.W., Levin, N.W., Kotanko, P., et al. (2012). Predictors of heart rate variability and its prognostic significance in chronic kidney disease. *Nephrol. Dial. Transpl.* 27**,** 700-709.

Chappey, O., Dosquet, C., Wautier, M.P., and Wautier, J.L. (1997). Advanced glycation end products, oxidant stress and vascular lesions. *Eur. J. Clin. Invest.* 27**,** 97-108.

Chen, A., Huang, B.S., Wang, H.W., Ahmad, M., and Leenen, F.H.H. (2014). Knockdown of mineralocorticoid or angiotensin II type 1 receptor gene expression in the paraventricular nucleus prevents angiotensin II hypertension in rats. *J. Physiol.* 592**,** 3523-3536.

Chen, A.D., Zhang, S.J., Yuan, N., Xu, Y., De, W., et al. (2011a). Angiotensin AT1 receptors in paraventricular nucleus contribute to sympathetic activation and enhanced cardiac sympathetic afferent reflex in renovascular hypertensive rats. *Exp. Physiol.* 96**,** 94-103.

Chen, F., Liu, F., and Badoer, E. (2011b). AT1 receptors in the paraventricular nucleus mediate the hyperthermia-induced reflex reduction of renal blood flow in rats. *Am. J. Physiol. Regul. Integr. Comp. Physiol.* 300**,** R479-485.

Chen, Q., and Pan, H.L. (2007). Signaling mechanisms of angiotensin II-induced attenuation of GABAergic input to hypothalamic presympathetic neurons. *J. Neurophysiol.* 97**,** 3279-3287.

Chen, Q.H., and Toney, G.M. (2010). In vivo discharge properties of hypothalamic paraventricular nucleus neurons with axonal projections to the rostral ventrolateral medulla. *J. Neurophysiol.* 103**,** 4-15.

Chen, R.Y., Fan, F.C., Schuessler, G.B., and Chien, S. (1982). Baroreflex control of heart rate in humans during nitroprusside-induced hypotension. *Am. J. Physiol. Regul. Integr. Comp. Physiol.* 243**,** R18-R24.

Chen, W.W., Xiong, X.Q., Chen, Q., Li, Y.H., Kang, Y.M., et al. (2015). Cardiac sympathetic afferent reflex and its implications for sympathetic activation in chronic heart failure and hypertension. *Acta. Physiol. (Oxf).* 213**,** 778-794.

Chen, Y.L., Chan, S.H., and Chan, J.Y. (1996). Participation of galanin in baroreflex inhibition of heart rate by hypothalamic PVN in rat. *Am. J. Physiol.* 271**,** H1823-1828.

Cheng, L.T., Gao, Y.L., Gu, Y., Zhang, L., Bi, S.H., et al. (2008). Stepwise increase in the prevalence of isolated systolic hypertension with the stages of chronic kidney disease. *Nephrol. Dial. Transplant.* 23**,** 3895-3900.

Ciriello, J. (1998). Afferent renal inputs to paraventricular nucleus vasopressin and oxytocin neurosecretory neurons. *Am. J. Physiol.* 275**,** R1745-1754.

Ciriello, J., and Calaresu, F.R. (1980a). Monosynaptic pathway from cardiovascular neurons in the nucleus tractus solitarii to the paraventricular nucleus in the cat. *Brain Res.* 193**,** 529-533.

Ciriello, J., and Calaresu, F.R. (1980b). Role of paraventricular and supraoptic nuclei in central cardiovascular regulation in the cat. *Am. J. Physiol.* 239**,** R137-142.

Ciriello, J., and Caverson, M.M. (1984). Ventrolateral medullary neurons relay cardiovascular inputs to the paraventricular nucleus. *Am. J. Physiol.* 246**,** R968-978.

Cox, B.F., Hay, M., and Bishop, V.S. (1990). Neurons in area postrema mediate vasopressin-induced enhancement of the baroreflex. *Am. J. Physiol.* 258**,** H1943-1946.

Crestani, C.C., Alves, F.H., Busnardo, C., Resstel, L.B., and Correa, F.M. (2010). N-methyl-D-aspartate glutamate receptors in the hypothalamic paraventricular nucleus modulate cardiac component of the baroreflex in unanesthetized rats. *Neurosci. Res.* 67**,** 317-326.

Csaki, A., Kocsis, K., Halasz, B., and Kiss, J. (2000). Localization of glutamatergic/aspartatergic neurons projecting to the hypothalamic paraventricular nucleus studied by retrograde transport of [3H]D-aspartate autoradiography. *Neuroscience* 101**,** 637-655.

Czaczkes, J.W., Kleeman, C.R., and Koenig, M. (1964). Physiologic studies of antidiuretic hormone by its direct measurement in human plasma. *J. Clin. Invest.* 43**,** 1625-1640.

Daftary, S.S., Boudaba, C., Szabo, K., and Tasker, J.G. (1998). Noradrenergic excitation of magnocellular neurons in the rat hypothalamic paraventricular nucleus via intranuclear glutamatergic circuits. *J. Neurosci.* 18**,** 10619-10628.

Dahlof, B. (1995). Effect of angiotensin II blockade on cardiac hypertrophy and remodelling: a review. *J. Hum. Hypertens.* 9 Suppl 5**,** S37-44.

Daly, M.B., and Kirkman, E. (1989). Differential modulation by pulmonary stretch afferents of some reflex cardioinhibitory responses in the cat. *J. Physiol.* 417**,** 323-341.

Danbolt, N.C. (2001). Glutamate uptake. *Prog. Neurobiol.* 65**,** 1-105.

De Campos, R.P., Siegel, J.M., Fresta, C.G., Caruso, G., Da Silva, J.A., et al. (2015). Indirect detection of superoxide in RAW 264.7 macrophage cells using microchip

electrophoresis coupled to laser-induced fluorescence. *Anal. Bioanal. Chem.* 407**,** 7003-7012.

De Nicola, L., Gabbai, F.B., Agarwal, R., Chiodini, P., Borrelli, S., et al. (2013). Prevalence and prognostic role of resistant hypertension in chronic kidney disease patients. *J. Am. Coll. Cardiol.* 61**,** 2461-2467.

Dibona, G.F. (2005). Physiology in perspective: the wisdom of the body. neural control of the kidney. *Am. J. Physiol. Regul. Integr. Comp. Physiol.* 289**,** R633-641.

Ding, A., Kalaignanasundaram, P., Ricardo, S.D., Abdelkader, A., Witting, P.K., et al. (2012). Chronic treatment with tempol does not significantly ameliorate renal tissue hypoxia or disease progression in a rodent model of polycystic kidney disease. *Clin. Exp. Pharmacol. Physiol.* 39**,** 917-929.

Duan, Y.F., Kopin, I.J., and Goldstein, D.S. (1999). Stimulation of the paraventricular nucleus modulates firing of neurons in the nucleus of the solitary tract. *Am. J. Physiol.* 277**,** R403-411.

Dufloth, D.L., Morris, M., and Michelini, L.C. (1997). Modulation of exercise tachycardia by vasopressin in the nucleus tractus solitarii. *Am. J. Physiol. Regul. Integr. Comp. Physiol.* 273**,** R1271-R1282.

Durocher, J.J., Klein, J.C., and Carter, J.R. (2011). Attenuation of sympathetic baroreflex sensitivity during the onset of acute mental stress in humans. *Am. J. Physiol. Heart Circ. Physiol.* 300**,** H1788-1793.

Faber, J.E. (1989). Effects of althesin and urethan-chloralose on neurohumoral cardiovascular regulation. *Am. J. Physiol.* 256**,** R757-765.

Farrell, T.G., Paul, V., Cripps, T.R., Malik, M., Bennett, E.D., et al. (1991). Baroreflex sensitivity and electrophysiological correlates in patients after acute myocardial infarction. *Circulation* 83**,** 945-952.

Franklin, S.S., and Wong, N.D. (2013). Hypertension and cardiovascular disease: contributions of the framingham heart study. *Global Heart* 8**,** 49-57.

Fujita, M., Ando, K., Kawarazaki, H., Kawarasaki, C., Muraoka, K., et al. (2012). Sympathoexcitation by brain oxidative stress mediates arterial pressure elevation in salt-induced chronic kidney disease. *Hypertension* 59**,** 105-112.

Gaede, A., and Pilowsky, P. (2013). "Excitatory responses to microinjection of glutamate depend on dose not volume: a meta-analysis of studies in rat RVLM," in *Stimulation and inhibition of neurons,* eds. P.M. Pilowsky, M.M.J. Farnham & A.Y. Fong. (New York City, NY: Humana Press), 37-46.

Gan, X.-B., Sun, H.-J., Chen, D., Zhang, L.-L., Zhou, H., et al. (2014). Intermedin in the paraventricular nucleus attenuates cardiac sympathetic afferent reflex in chronic heart failure rats. *PLoS One* 9**,** e94234.

Geraldes, V., Goncalves-Rosa, N., Liu, B., Paton, J.F., and Rocha, I. (2014). Chronic depression of hypothalamic paraventricular neuronal activity produces sustained hypotension in hypertensive rats. *Exp. Physiol.* 99**,** 89-100.

Glass, M.J., Wang, G., Coleman, C.G., Chan, J., Ogorodnik, E., et al. (2015). NMDA receptor plasticity in the hypothalamic paraventricular nucleus contributes to the elevated blood pressure produced by angiotensin II. *J. Neurosci.* 35**,** 9558-9567.

Grassi, G., Cattaneo, B.M., Seravalle, G., Lanfranchi, A., and Mancia, G. (1998). Baroreflex control of sympathetic nerve activity in essential and secondary hypertension. *Hypertension* 31**,** 68-72.

Grassi, G., Quarti-Trevano, F., Seravalle, G., Arenare, F., Volpe, M., et al. (2011). Early sympathetic activation in the initial clinical stages of chronic renal failure. *Hypertension* 57**,** 846-851.

Grassi, G., Seravalle, G., Arenare, F., Buccianti, G., Furiani, S., et al. (2009). Behaviour of regional adrenergic outflow in mild-to-moderate renal failure. *J. Hypertens.* 27**,** 562-566.

Grimm, D.R. (1997). Neurally mediated syncope: a review of cardiac and arterial receptors. *J. Clin. Neurophysiol.* 14**,** 170-182.

Guggilam, A., Cardinale, J.P., Mariappan, N., Sriramula, S., Haque, M., et al. (2011). Central TNF inhibition results in attenuated neurohumoral excitation in heart failure: a role for superoxide and nitric oxide. *Basic Res. Cardiol.* 106**,** 273-286.

Guyenet, P.G. (2006). The sympathetic control of blood pressure. *Nat. Rev. Neurosci.* 7**,** 335-346.

Han, Y., Shi, Z., Zhang, F., Yu, Y., Zhong, M.K., et al. (2007). Reactive oxygen species in the paraventricular nucleus mediate the cardiac sympathetic afferent reflex in chronic heart failure rats. *Eur. J. Heart Fail.* 9**,** 967-973.

Head, G.A., Saigusa, T., and Mayorov, D.N. (2002). Angiotensin and baroreflex control of the circulation. *Braz. J. Med. Biol. Res.* 35**,** 1047-1059.

Hering, D., Mahfoud, F., Walton, A.S., Krum, H., Lambert, G.W., et al. (2012). Renal denervation in moderate to severe CKD. *J. Am. Soc. Nephrol.* 23**,** 1250-1257.

Hering, D., and Schlaich, M. (2015). The role of central nervous system mechanisms in resistant hypertension. *Curr. Hypertens. Rep.* 17**,** 58.

Higa, K.T., Mori, E., Viana, F.F., Morris, M., and Michelini, L.C. (2002). Baroreflex control of heart rate by oxytocin in the solitary-vagal complex. *Am. J. Physiol. Regul. Integr. Comp. Physiol.* 282**,** R537-R545.

Hildreth, C.M., Kandukuri, D.S., Goodchild, A.K., and Phillips, J.K. (2013). Temporal development of baroreceptor dysfunction in a rodent model of chronic kidney disease. *Clin. Exp. Pharmacol. Physiol.* 40**,** 458-465.

Hildreth, C.M., and Phillips, J.K. (2014). "Enhanced glutamatergic inputs to paraventricular nucleus of the hypothalamus contribute to increase blood pressure and sympathetic nerve activity in chronic kidney disease", in: *Meeting of the australasian neuroscience society*: Unpublished conference paper.

Hohnloser, S.H., Klingenheben, T., Van De Loo, A., Hablawetz, E., Just, H., et al. (1994). Reflex versus tonic vagal activity as a prognostic parameter in patients with sustained ventricular tachycardia or ventricular fibrillation. *Circulation* 89**,** 1068-1073.

Hollenberg, N.K. (1999). Pharmacologic interruption of the renin-angiotensin system and the kidney: differential responses to angiotensin-converting enzyme and renin inhibition. *J. Am. Soc. Nephrol.* 10 Suppl 11**,** S239-242.

Holmes, C.L., Patel, B.M., Russell, J.A., and Walley, K.R. (2001). Physiology of vasopressin relevant to management of septic shock. *Chest* 120**,** 989-1002.

Holobotovskyy, V.V., Arnolda, L.F., and Mckitrick, D.J. (2004). Effect of anaesthetic and rat strain on heart rate responses to simulated haemorrhage. *Acta Physiol. Scand.* 180**,** 29-38.

Huang, B.S., Chen, A., Ahmad, M., Wang, H.W., and Leenen, F.H. (2014). Mineralocorticoid and AT1 receptors in the paraventricular nucleus contribute to sympathetic hyperactivity and cardiac dysfunction in rats post myocardial infarct. *J. Physiol.* 592**,** 3273-3286.

Huber, D.A., and Schreihofer, A.M. (2010). Attenuated baroreflex control of sympathetic nerve activity in obese Zucker rats by central mechanisms. *J. Physiol.* 588**,** 1515-1525.

Huddleston, A.T., Tang, W., Takeshima, H., Hamilton, S.L., and Klann, E. (2008). Superoxide-induced potentiation in the hippocampus requires activation of ryanodine receptor type 3 and ERK. *J. Neurophysiol.* 99**,** 1565-1571.

Ibrahim, J., Berk, B.C., and Hughes, A.D. (2006). Comparison of simultaneous measurements of blood pressure by tail-cuff and carotid arterial methods in conscious spontaneously hypertensive and Wistar-Kyoto rats. *Clin. Exp. Hypertens.* 28**,** 57-72.

Infanger, D.W., Sharma, R.V., and Davisson, R.L. (2006). NADPH oxidases of the brain: distribution, regulation, and function. *Antioxidants & redox signaling* 8**,** 1583-1596.

Ishii, M., Ikeda, T., Takagi, M., Sugimoto, T., Atarashi, K., et al. (1983). Elevated plasma catecholamines in hypertensives with primary glomerular diseases. *Hypertension* 5**,** 545-551.

Jancovski, N., Bassi, J.K., Carter, D.A., Choong, Y.T., Connelly, A., et al. (2013). Stimulation of angiotensin type 1A receptors on catecholaminergic cells contributes to angiotensin-dependent hypertension. *Hypertension* 62**,** 866-871.

Jeewandara, T.M., Ameer, O.Z., Boyd, R., Wyse, B.F., Underwood, C.F., et al. (2015). Protective cardiorenal effects of spironolactone in a rodent model of polycystic kidney disease. *Clin. Exp. Pharmacol. Physiol.* 42**,** 353-360.

Jensen, E.C. (2013). Quantitative analysis of histological staining and fluorescence using ImageJ. *Anat. Rec.* 296**,** 378-381.

Jin, C.B., and Rockhold, R.W. (1989). Effects of paraventricular hypothalamic microinfusions of kainic acid on cardiovascular and renal excretory function in conscious rats. *J. Pharmacol. Exp. Ther.* 251**,** 969-975.

Johansson, M., Gao, S.A., Friberg, P., Annerstedt, M., Carlstrom, J., et al. (2007). Baroreflex effectiveness index and baroreflex sensitivity predict all-cause mortality and sudden death in hypertensive patients with chronic renal failure. *J. Hypertens.* 25**,** 163-168.

John, S.G., Sigrist, M.K., and Mcintyre, C.W. (Year). "Impaired baroreflex sensitivity predicts mortality in chronic kidney disease", in: *Computers in Cardiology, 2008*: Computers in Cardiology), 745-748.

Judy, W.V., Watanabe, A.M., Henry, D.P., Besch, H.R., Jr., Murphy, W.R., et al. (1976). Sympathetic nerve activity: role in regulation of blood pressure in the spontaenously hypertensive rat. *Circ. Res.* 38**,** 21-29.

Jung, R., Bruce, E.N., and Katona, P.G. (1991). Cardiorespiratory responses to glutamatergic antagonists in the caudal ventrolateral medulla of rats. *Brain Res.* 564**,** 286-295.

Kalyanaraman, B., Dranka, B.P., Hardy, M., Michalski, R., and Zielonka, J. (2014). HPLC-based monitoring of products formed from hydroethidine-based fluorogenic probes--the ultimate approach for intra- and extracellular superoxide detection. *Biochim. Biophys. Acta* 1840**,** 739-744.

Kawabe, T., Chitravanshi, V.C., Nakamura, T., Kawabe, K., and Sapru, H.N. (2009). Mechanism of heart rate responses elicited by chemical stimulation of the hypothalamic paraventricular nucleus in the rat. *Brain Res.* 1248**,** 115-126.

Keith, D.S., Nichols, G.A., Gullion, C.M., Brown, J.B., and Smith, D.H. (2004). Longitudinal follow-up and outcomes among a population with chronic kidney disease in a large managed care organization. *Arch. Intern. Med.* 164**,** 659-663.

Keith, D.S., Torres, V.E., Johnson, C.M., and Holley, K.E. (1994). Effect of sodium chloride, enalapril, and losartan on the development of polycystic kidney disease in Han:SPRD rats. *Am. J. Kidney Dis.* 24**,** 491-498.

Kent, B.B., Drane, J.W., Blumenstein, B., and Manning, J.W. (1972). A mathematical model to assess changes in the baroreceptor reflex. *Cardiology* 57**,** 295-310.

Kiuchi, M.G., Maia, G.L.M., De Queiroz Carreira, M.a.M., Kiuchi, T., Chen, S., et al. (2013). Effects of renal denervation with a standard irrigated cardiac ablation catheter on blood pressure and renal function in patients with chronic kidney disease and resistant hypertension. *Eur. Heart J.* 34**,** 2114-2121.

Klahr, S., Levey, A.S., Beck, G.J., Caggiula, A.W., Hunsicker, L., et al. (1994). The effects of dietary protein restriction and blood-pressure control on the progression of chronic renal disease. *N. Engl. J. Med.* 330**,** 877-884.

Klann, E. (1998). Cell-permeable scavengers of superoxide prevent long-term potentiation in hippocampal area CA1. *J. Neurophysiol.* 80**,** 452-457.

Klein, I.H., Ligtenberg, G., Neumann, J., Oey, P.L., Koomans, H.A., et al. (2003a). Sympathetic nerve activity is inappropriately increased in chronic renal disease. *J. Am. Soc. Nephrol.* 14**,** 3239-3244.

Klein, I.H., Ligtenberg, G., Oey, P.L., Koomans, H.A., and Blankestijn, P.J. (2001). Sympathetic activity is increased in polycystic kidney disease and is associated with hypertension. *J. Am. Soc. Nephrol.* 12**,** 2427-2433.

Klein, I.H., Ligtenberg, G., Oey, P.L., Koomans, H.A., and Blankestijn, P.J. (2003b). Enalapril and losartan reduce sympathetic hyperactivity in patients with chronic renal failure. *J. Am. Soc. Nephrol.* 14**,** 425-430.

Krauhs, J. (1979). Structure of rat aortic baroreceptors and their relationship to connective tissue. *J. Neurocytol.* 8**,** 401-414.

Krieger, E.M. (1988). Mechanisms of complete baroreceptor resetting in hypertension. *Drugs* 35 Suppl 6**,** 98-103.

Kubo, T., and Kihara, M. (1990). Modulation of the aortic baroreceptor reflex by neuropeptide Y, neurotensin and vasopressin microinjected into the nucleus tractus solitarii of the rat. *Naunyn Schmiedebergs Arch. Pharmacol.* 342**,** 182-188.

Kwon, T.H., Chao, D.L., Malloy, K., Sun, D., Alessandri, B., et al. (2003). Tempol, a novel stable nitroxide, reduces brain damage and free radical production, after acute subdural hematoma in the rat. *J. Neurotrauma* 20**,** 337-345.

La Rovere, M.T., Specchia, G., Mortara, A., and Schwartz, P.J. (1988). Baroreflex sensitivity, clinical correlates, and cardiovascular mortality among patients with a first myocardial infarction. A prospective study. *Circulation* 78**,** 816-824.

Lacy, P., Carr, S.J., O'brien, D., Fentum, B., Williams, B., et al. (2006). Reduced glomerular filtration rate in pre-dialysis non-diabetic chronic kidney disease patients is associated with impaired baroreceptor sensitivity and reduced vascular compliance. *Clin. Sci.* 110**,** 101-108.

Leng, G., Brown, C.H., and Russell, J.A. (1999). Physiological pathways regulating the activity of magnocellular neurosecretory cells. *Prog. Neurobiol.* 57**,** 625-655.

Lenkei, Z., Corvol, P., and Llorens-Cortes, C. (1995). The angiotensin receptor subtype AT1A predominates in rat forebrain areas involved in blood pressure, body fluid homeostasis and neuroendocrine control. *Mol. Brain Res.* 30**,** 53-60.

Levey, A.S., Eckardt, K.U., Tsukamoto, Y., Levin, A., Coresh, J., et al. (2005). Definition and classification of chronic kidney disease: A position statement from Kidney Disease: Improving Global Outcomes (KDIGO). *Kidney Int.* 67**,** 2089-2100.

Li, D.-P., and Pan, H.-L. (2007a). Glutamatergic inputs in the hypothalamic paraventricular nucleus maintain sympathetic vasomotor tone in hypertension. *Hypertension* 49**,** 916-925.

Li, D.P., Chen, S.R., Finnegan, T.F., and Pan, H.L. (2004). Signalling pathway of nitric oxide in synaptic GABA release in the rat paraventricular nucleus. *J. Physiol.* 554**,** 100-110.

Li, D.P., Chen, S.R., and Pan, H.L. (2003a). Angiotensin II stimulates spinally projecting paraventricular neurons through presynaptic disinhibition. *J. Neurosci.* 23**,** 5041-5049.

Li, D.P., and Pan, H.L. (2005). Angiotensin II attenuates synaptic GABA release and excites paraventricular-rostral ventrolateral medulla output neurons. *J. Pharmacol. Exp. Ther.* 313**,** 1035-1045.

Li, D.P., and Pan, H.L. (2007b). Role of gamma-aminobutyric acid (GABA)A and GABAB receptors in paraventricular nucleus in control of sympathetic vasomotor tone in hypertension. *J. Pharmacol. Exp. Ther.* 320**,** 615-626.

Li, Y.-F., Cornish, K.G., and Patel, K.P. (2003b). Alteration of NMDA NR1 receptors within the paraventricular nucleus of hypothalamus in rats with heart failure. *Circ. Res.* 93**,** 990-997.

Li, Y.F., Jackson, K.L., Stern, J.E., Rabeler, B., and Patel, K.P. (2006). Interaction between glutamate and GABA systems in the integration of sympathetic outflow by the paraventricular nucleus of the hypothalamus. *Am. J. Physiol. Heart Circ. Physiol.* 291**,** H2847-2856.

Li, Z., Bains, J.S., and Ferguson, A.V. (1993). Functional evidence that the angiotensin antagonist losartan crosses the blood-brain barrier in the rat. *Brain Res. Bull.* 30**,** 33-39.

Ligtenberg, G., Blankestijn, P.J., Oey, P.L., Klein, I.H.H., Dijkhorst-Oei, L.-T., et al. (1999). Reduction of sympathetic hyperactivity by enalapril in patients with chronic renal failure. *N. Engl. J. Med.* 340**,** 1321-1328.

Lind, R.W., Swanson, L.W., and Ganten, D. (1985). Organization of angiotensin II immunoreactive cells and fibers in the rat central nervous system. An immunohistochemical study. *Neuroendocrinology* 40**,** 2-24.

Liu, D., Gao, L., Roy, S.K., Cornish, K.G., and Zucker, I.H. (2008). The role of oxidant stress on AT1 receptor expression in neurons of rabbits with heart failure and in cultured neurons. *Circ. Res.* 103**,** 186-193.

Loewy, A.D. (1990). "Central autonomic pathways," in *Central Regulation of Autonomic Functions*, ed. A.D. Loewy. (New York City, NY: Oxford University Press), 88-103.

Martins-Pinge, M.C., Mueller, P.J., Foley, C.M., Heesch, C.M., and Hasser, E.M. (2012). Regulation of arterial pressure by the paraventricular nucleus in conscious rats: interactions among glutamate, GABA, and nitric oxide. *Front. Physiol.* 3**,** 490.

Massaad, C.A., and Klann, E. (2011). Reactive oxygen species in the regulation of synaptic plasticity and memory. *Antioxid. Redox Signal.* 14**,** 2013-2054.

Masson, G.S., Costa, T.S., Yshii, L., Fernandes, D.C., Soares, P.P., et al. (2014). Time-dependent effects of training on cardiovascular control in spontaneously hypertensive rats: role for brain oxidative stress and inflammation and baroreflex sensitivity. *PLoS One* 9**,** e94927.

Mcallen, R.M., and Spyer, K.M. (1978). The baroreceptor input to cardiac vagal motoneurones. *J. Physiol* 282**,** 365-374.

Mccooke, J., Appels, R., Barrero, R., Ding, A., Ozimek-Kulik, J., et al. (2012). A novel mutation causing nephronophthisis in the Lewis polycystic kidney rat localises to a conserved RCC1 domain in Nek8. *BMC Genomics* 13**,** 1-17.

Mccubbin, J.W., Green, J.H., and Page, I.H. (1956). Baroceptor function in chronic renal hypertension. *Circ. Res.* 4**,** 205-210.

Menon, V., Gul, A., and Sarnak, M.J. (2005). Cardiovascular risk factors in chronic kidney disease. *Kidney Int.* 68**,** 1413-1418.

Michelini, L.C., and Bonagamba, L.G. (1988). Baroreceptor reflex modulation by vasopressin microinjected into the nucleus tractus solitarii of conscious rats. *Hypertension* 11**,** I75-79.

Michelini, L.C., and Stern, J.E. (2009). Exercise-induced neuronal plasticity in central autonomic networks: role in cardiovascular control. *Exp. Physiol.* 94**,** 947-960.

Miller, M.E., Davidge, S.T., and Mitchell, B.F. (2002). Oxytocin does not directly affect vascular tone in vessels from nonpregnant and pregnant rats. *Am. J. Physiol. Heart Circ. Physiol.* 282**,** H1223-1228.

Moraes, D.J., Machado, B.H., and Paton, J.F. (2014). Specific respiratory neuron types have increased excitability that drive presympathetic neurones in neurogenic hypertension. *Hypertension* 63**,** 1309-1318.

Mortara, A., La Rovere, M.T., Pinna, G.D., Prpa, A., Maestri, R., et al. (1997). Arterial baroreflex modulation of heart rate in chronic heart failure: clinical and hemodynamic correlates and prognostic implications. *Circulation* 96**,** 3450-3458.

Morton, J.J., Beattie, E.C., and Macpherson, F. (1992). Angiotensin II receptor antagonist losartan has persistent effects on blood pressure in the young spontaneously hypertensive rat: lack of relation to vascular structure. *J. Vasc. Res.* 29**,** 264-269.

Moyses, M.R., Cabral, A.M., Bissoli, N., and Vasquez, E.C. (1994). Time course of changes in sigmoidal-fitting baroreceptor curves in one-kidney, one clip hypertensive rats. *Hypertension* 23**,** I87-92.

Ng, G.A., Brack, K.E., and Coote, J.H. (2001). Effects of direct sympathetic and vagus nerve stimulation on the physiology of the whole heart--a novel model of isolated Langendorff perfused rabbit heart with intact dual autonomic innervation. *Exp. Physiol.* 86**,** 319-329.

Ng, K., Hildreth, C.M., Avolio, A.P., and Phillips, J.K. (2011a). Angiotensin-converting enzyme inhibitor limits pulse-wave velocity and aortic calcification in a rat model of cystic renal disease. *Am. J. Physiol. Renal Physiol.* 301**,** F959-F966.

Ng, K., Hildreth, C.M., Phillips, J.K., and Avolio, A.P. (2011b). Aortic stiffness is associated with vascular calcification and remodeling in a chronic kidney disease rat model. *Am. J. Physiol. Renal Physiol.* 300**,** F1431-F1436.

Nicholson, C. (1985). Diffusion from an injected volume of a substance in brain tissue with arbitrary volume fraction and tortuosity. *Brain Res* 333**,** 325-329.

Nishi, E.E., Oliveira-Sales, E.B., Bergamaschi, C.T., Oliveira, T.G., Boim, M.A., et al. (2010). Chronic antioxidant treatment improves arterial renovascular hypertension and oxidative stress markers in the kidney in Wistar rats. *Am. J. Hypertens.* 23**,** 473-480.

Noor, R., Mittal, S., and Iqbal, J. (2002). Superoxide dismutase-applications and relevance to human diseases. *Med. Sci. Monit.* 8**,** Ra210-215.

Oparil, S., Chen, Y.F., Peng, N., and Wyss, J.M. (1996). Anterior hypothalamic norepinephrine, atrial natriuretic peptide, and hypertension. *Front. Neuroendocrinol.* 17**,** 212-246.

Osborn, J.W., and Fink, G.D. (2010). Region-specific changes in sympathetic nerve activity in angiotensin II-salt hypertension in the rat. *Exp. Physiol.* 95**,** 61-68.

Palkovits, M., Sebekova, K., Klenovics, K.S., Kebis, A., Fazeli, G., et al. (2013). Neuronal activation in the central nervous system of rats in the initial stage of chronic kidney disease-modulatory effects of losartan and moxonidine. *PLoS One* 8**,** e66543.

Pannirselvam, M., Wiehler, W.B., Anderson, T., and Triggle, C.R. (2005). Enhanced vascular reactivity of small mesenteric arteries from diabetic mice is associated with enhanced oxidative stress and cyclooxygenase products. *Br. J. Pharmacol.* 144**,** 953-960.

Park, J., Campese, V.M., Nobakht, N., and Middlekauff, H.R. (2008). Differential distribution of muscle and skin sympathetic nerve activity in patients with end-stage renal disease. *J. Appl. Physiol.* 105**,** 1873-1876.

Parlow, J., Viale, J.P., Annat, G., Hughson, R., and Quintin, L. (1995). Spontaneous cardiac baroreflex in humans. Comparison with drug-induced responses. *Hypertension* 25**,** 1058-1068.

Patel, K.P., Mayhan, W.G., Bidasee, K.R., and Zheng, H. (2011). Enhanced angiotensin II-mediated central sympathoexcitation in streptozotocin-induced diabetes: role of superoxide anion. *Am. J. Physiol. Regul. Integr. Comp. Physiol.* 300**,** R311-320.

Patel, K.P., Salgado, H.C., Liu, X., and Zheng, H. (2013). Exercise training normalizes the blunted central component of the baroreflex in rats with heart failure: role of the PVN. *Am. J. Physiol. Heart Circ. Physiol.* 305**,** H173-181.

Patel, K.P., and Schmid, P.G. (1988). Role of paraventricular nucleus (PVH) in baroreflex-mediated changes in lumbar sympathetic nerve activity and heart rate. *J. Auton. Nerv. Syst.* 22**,** 211-219.

Paxinos, G., and Watson, C. (2013). *The rat brain in stereotaxic coordinates, 7th edition.* Waltham, MA: Elsevier Science.

Peters, J.H., Mcdougall, S.J., Kellett, D.O., Jordan, D., Llewellyn-Smith, I.J., et al. (2008). Oxytocin enhances cranial visceral afferent synaptic transmission to the solitary tract nucleus. *J. Neurosci.* 28**,** 11731-11740.

Phillips, J.K., Hopwood, D., Loxley, R.A., Ghatora, K., Coombes, J.D., et al. (2007). Temporal relationship between renal cyst development, hypertension and cardiac hypertrophy in a new rat model of autosomal recessive polycystic kidney disease. *Kidney Blood Press. Res.* 30**,** 129-144.

Pickering, A.E., Boscan, P., and Paton, J.F.R. (2003). Nociception attenuates parasympathetic but not sympathetic baroreflex via NK(1) receptors in the rat nucleus tractus solitarii. *J. Physiol.* 551**,** 589-599.

Pilowsky, P.M., and Goodchild, A.K. (2002). Baroreceptor reflex pathways and neurotransmitters: 10 years on. *J. Hypertens.* 20**,** 1675-1688.

Pinol, R.A., Jameson, H., Popratiloff, A., Lee, N.H., and Mendelowitz, D. (2014). Visualization of oxytocin release that mediates paired pulse facilitation in hypothalamic pathways to brainstem autonomic neurons. *PLoS One* 9**,** e112138.

Potapenko, E.S., Biancardi, V.C., Zhou, Y., and Stern, J.E. (2012). Altered astrocyte glutamate transporter regulation of hypothalamic neurosecretory neurons in heart failure rats. *Am. J. Physiol. Regul. Integr. Comp. Physiol.* 303**,** R291-300.

Pyner, S. (2009). Neurochemistry of the paraventricular nucleus of the hypothalamus: implications for cardiovascular regulation. *J. Chem. Neuroanat.* 38**,** 197-208.

Queiroz, E.A., Okada, M.N., Fumega, U., Fontes, M.A., Moraes, M.F., et al. (2011). Excitatory amino acid receptors in the dorsomedial hypothalamus are involved in the cardiovascular and behavioural chemoreflex responses. *Exp. Physiol.* 96**,** 73-84.

Rahn, K.H., Heidenreich, S., and Bruckner, D. (1999). How to assess glomerular function and damage in humans. *J. Hypertens.* 17**,** 309-317.

Rinaman, L. (1998). Oxytocinergic inputs to the nucleus of the solitary tract and dorsal motor nucleus of the vagus in neonatal rats. *J. Comp. Neurol.* 399**,** 101-109.

Rockhold, R.W., Acuff, C.G., and Clower, B.R. (1990). Excitotoxic lesions of the paraventricular hypothalamus: metabolic and cardiac effects. *Neuropharmacology* 29**,** 663-673.

Sadoshima, J., and Izumo, S. (1993). Molecular characterization of angiotensin II--induced hypertrophy of cardiac myocytes and hyperplasia of cardiac fibroblasts. Critical role of the AT1 receptor subtype. *Circ. Res.* 73**,** 413-423.

Sakai, K., Agassandian, K., Morimoto, S., Sinnayah, P., Cassell, M.D., et al. (2007). Local production of angiotensin II in the subfornical organ causes elevated drinking. *J. Clin. Invest.* 117**,** 1088-1095.

Saleh, T.M., and Connell, B.J. (2000). 17beta-estradiol modulates baroreflex sensitivity and autonomic tone of female rats. *J. Auton. Nerv. Syst.* 80**,** 148-161.

Salgado, H.C., Barale, A.R., Castania, J.A., Machado, B.H., Chapleau, M.W., et al. (2007). Baroreflex responses to electrical stimulation of aortic depressor nerve in conscious SHR. *Am. J. Physiol. Heart Circ. Physiol.* 292**,** H593-600.

Salgado, H.C., and Krieger, E.M. (1988). Extent of baroreceptor resetting in response to sodium nitroprusside and verapamil. *Hypertension* 11**,** I121-125.

Salman, I.M. (2014). *Cardiovascular autonomic dysfunction in chronic kidney disease.* Doctoral Thesis, Sydney, Australia : Macquarie University.

Salman, I.M., Hildreth, C.M., Ameer, O.Z., and Phillips, J.K. (2014). Differential contribution of afferent and central pathways to the development of baroreflex dysfunction in chronic kidney disease. *Hypertension* 63**,** 804-810.

Salman, I.M., Phillips, J.K., Ameer, O.Z., and Hildreth, C.M. (2015a). Abnormal central control underlies impaired baroreflex control of heart rate and sympathetic nerve activity in female Lewis polycystic kidney rats. *J. Hypertens.* 33**,** 1418-1428.

Salman, I.M., Sarma Kandukuri, D., Harrison, J.L., Hildreth, C.M., and Phillips, J.K. (2015b). Direct conscious telemetry recordings demonstrate increased renal sympathetic nerve activity in rats with chronic kidney disease. *Front. Physiol.* 6**,** 218.

Sapru, H.N., and Wang, S.C. (1976). Modification of aortic barorecptor resetting in the spontaneously hypertensive rat. *Am. J. Physiol.* 230**,** 664-674.

Schwartz, J., and Reid, I.A. (1981). Effect of vasopressin blockade on blood pressure regulation during hemorrhage in conscious dogs. *Endocrinology* 109**,** 1778-1780.

Shafton, A.D., Ryan, A., and Badoer, E. (1998). Neurons in the hypothalamic paraventricular nucleus send collaterals to the spinal cord and to the rostral ventrolateral medulla in the rat. *Brain Res.* 801**,** 239-243.

Sharpe, A.L., Calderon, A.S., Andrade, M.A., Cunningham, J.T., Mifflin, S.W., et al. (2013). Chronic intermittent hypoxia increases sympathetic control of blood pressure: role of neuronal activity in the hypothalamic paraventricular nucleus. *Am. J. Physiol. Heart Circ. Physiol.* 305**,** H1772-1780.

Shen, X.Z., Li, Y., Li, L., Shah, K.H., Bernstein, K.E., et al. (2015). Microglia participate in neurogenic regulation of hypertension. *Hypertension* 66**,** 309-316.

Shibasaki, Y., Masaki, H., Nishiue, T., Nishikawa, M., Matsubara, H., et al. (2002). Angiotensin II type 1 receptor antagonist, losartan, causes regression of left ventricular hypertrophy in end-stage renal disease. *Nephron* 90**,** 256-261.

Shih, C.D., Chan, S.H., and Chan, J.Y. (1995). Participation of hypothalamic paraventricular nucleus in locus ceruleus-induced baroreflex suppression in rats. *Am. J. Physiol.* 269**,** H46-52.

Shimokawa, A., Kunitake, T., Takasaki, M., and Kannan, H. (1998). Differential effects of anesthetics on sympathetic nerve activity and arterial baroreceptor reflex in chronically instrumented rats. *J. Auton. Nerv. Syst.* 72**,** 46-54.

Siddiqi, L., Prakken, N.H., Velthuis, B.K., Cramer, M.J., Oey, P.L., et al. (2010). Sympathetic activity in chronic kidney disease patients is related to left ventricular mass despite antihypertensive treatment. *Nephrol. Dial. Transplant.* 25**,** 3272-3277.

Sladek, C.D., Blair, M.L., and Mangiapane, M. (1987). Evidence against a pressor role for vasopressin in spontaneous hypertension. *Hypertension* 9**,** 332-338.

Stocker, S.D., Hunwick, K.J., and Toney, G.M. (2005). Hypothalamic paraventricular nucleus differentially supports lumbar and renal sympathetic outflow in water-deprived rats. *J. Physiol.* 563**,** 249-263.

Stocker, S.D., Keith, K.J., and Toney, G.M. (2004). Acute inhibition of the hypothalamic paraventricular nucleus decreases renal sympathetic nerve activity and arterial blood pressure in water-deprived rats. *Am. J. Physiol. Regul. Integr. Comp. Physiol.* 286**,** R719-725.

Strack, A.M., Sawyer, W.B., Hughes, J.H., Platt, K.B., and Loewy, A.D. (1989). A general pattern of CNS innervation of the sympathetic outflow demonstrated by transneuronal pseudorabies viral infections. *Brain Res.* 491**,** 156-162.

Streeter, E., Al-Magableh, M., Hart, J.L., and Badoer, E. (2011). Hydrogen sulfide in the RVLM and PVN has no effect on cardiovascular regulation. *Front. Physiol.* 2.

Stuesse, S.L., and Fish, S.E. (1984). Projections to the cardioinhibitory region of the nucleus ambiguus of rat. *J. Comp. Neurol.* 229**,** 271-278.

Su, Q., Qin, D.N., Wang, F.X., Ren, J., Li, H.B., et al. (2014). Inhibition of reactive oxygen species in hypothalamic paraventricular nucleus attenuates the renin-angiotensin system and proinflammatory cytokines in hypertension. *Toxicol. Appl. Pharmacol.* 276**,** 115-120.

Sun, H.-J., Li, P., Chen, W.-W., Xiong, X.-Q., and Han, Y. (2012). Angiotensin II and angiotensin-(1-7) in paraventricular nucleus modulate cardiac sympathetic afferent reflex in renovascular hypertensive rats. *PLoS One* 7**,** e52557.

Swanson, L.W., and Kuypers, H.G. (1980). The paraventricular nucleus of the hypothalamus: cytoarchitectonic subdivisions and organization of projections to the pituitary dorsal vagal complex and spinal cord as demonstrated by retrograde fluorescence double labeling methods. *J. Comp. Neurol.* 194**,** 555-570.

Swenne, C.A. (2013). Baroreflex sensitivity: mechanisms and measurement. *Neth. Heart J.* 21**,** 58-60.

Syková, E., and Nicholson, C. (2008). Diffusion in brain extracellular space. *Physiol. Rev.* 88**,** 1277-1340.

Takeda, K., Nakamura, Y., Okajima, H., Hayashi, J., Kawasaki, S., et al. (1988). Attenuated cardiovascular and sympathetic nerve responses to aortic nerve stimulation in DOCA-salt hypertensive rats. *J. Hypertens.* 6**,** 559-563.

Takeda, K., Nakata, T., Takesako, T., Itoh, H., Hirata, M., et al. (1991). Sympathetic inhibition and attenuation of spontaneous hypertension by PVN lesions in rats. *Brain Res.* 543**,** 296-300.

Thomas, G.D. (2011). Neural control of the circulation. *Adv. Physiol. Educ.* 35**,** 28-32.

Thompson, C.J., Bland, J., Burd, J., and Baylis, P.H. (1986). The osmotic thresholds for thirst and vasopressin release are similar in healthy man. *Clin. Sci. (Lond.)* 71**,** 651-656.

Tinucci, T., Abrahao, S.B., Santello, J.L., and Mion, D., Jr. (2001). Mild chronic renal insufficiency induces sympathetic overactivity. *J. Hum. Hypertens.* 15**,** 401-406.

Torres, V.E., Abebe, K.Z., Chapman, A.B., Schrier, R.W., Braun, W.E., et al. (2014). Angiotensin blockade in late autosomal dominant polycystic kidney disease. *N. Engl. J. Med.* 371**,** 2267-2276.

Tozawa, M., Iseki, K., Iseki, C., Kinjo, K., Ikemiya, Y., et al. (2003). Blood pressure predicts the risk of developing end-stage renal disease in men and women. *Hypertension* 41**,** 1341-1345.

Tremoleda, J.L., Kerton, A., and Gsell, W. (2012). Anaesthesia and physiological monitoring during in vivo imaging of laboratory rodents: considerations on experimental outcomes and animal welfare. *EJNMMI Res.* 2**,** 44.

Ullian, M.E. (1999). The role of corticosteriods in the regulation of vascular tone. *Cardiovasc. Res.* 41**,** 55-64.

Ulrich-Lai, Y.M., Jones, K.R., Ziegler, D.R., Cullinan, W.E., and Herman, J.P. (2011). Forebrain origins of glutamatergic innervation to the rat paraventricular nucleus of the hypothalamus: differential inputs to the anterior versus posterior subregions. *J. Comp. Neurol.* 519**,** 1301-1319.

Undesser, K.P., Lynn, M.P., and Bishop, V.S. (1984). Rapid resetting of aortic nerves in conscious rabbits. *Am. J. Physiol.* 246**,** H302-305.

Van Der Velde, M., Matsushita, K., Coresh, J., Astor, B.C., Woodward, M., et al. (2011). Lower estimated glomerular filtration rate and higher albuminuria are associated with all-cause and cardiovascular mortality. A collaborative meta-analysis of high-risk population cohorts. *Kidney Int.* 79**,** 1341-1352.

Van Houten, M., Schiffrin, E.L., Mann, J.F., Posner, B.I., and Boucher, R. (1980). Radioautographic localization of specific binding sites for blood-borne angiotensin II in the rat brain. *Brain Res.* 186**,** 480-485.

Vasavada, N., and Agarwal, R. (2003). Role of excess volume in the pathophysiology of hypertension in chronic kidney disease. *Kidney Int.* 64**,** 1772-1779.

Vissing, S.F., Scherrer, U., and Victor, R.G. (1989). Relation between sympathetic outflow and vascular resistance in the calf during perturbations in central venous pressure. Evidence for cardiopulmonary afferent regulation of calf vascular resistance in humans. *Circ. Res.* 65**,** 1710-1717.

Volterra, A., Trotti, D., Tromba, C., Floridi, S., and Racagni, G. (1994). Glutamate uptake inhibition by oxygen free radicals in rat cortical astrocytes. *J. Neurosci.* 14**,** 2924-2932.

Wang, G., Coleman, C.G., Chan, J., Faraco, G., Marques-Lopes, J., et al. (2013). Angiotensin II slow-pressor hypertension enhances NMDA currents and NOX2-dependent superoxide production in hypothalamic paraventricular neurons. *Am. J. Physiol. Regul. Integr. Comp. Physiol.* 304**,** R1096-1106.

Wang, G.F., Mao, X.J., and Chen, Z.J. (2014). Urethane suppresses renal sympathetic nerve activity in Wistar rats. *Eur. Rev. Med. Pharmacol. Sci.* 18**,** 1454-1457.

Wang, H.J., Zhang, F., Zhang, Y., Gao, X.Y., Wang, W., et al. (2005). AT1 receptor in paraventricular nucleus mediates the enhanced cardiac sympathetic afferent reflex in rats with chronic heart failure. *Auton. Neurosci.* 121**,** 56-63.

Wang, J., Irnaten, M., Venkatesan, P., Evans, C., and Mendelowitz, D. (2002). Arginine vasopressin enhances GABAergic inhibition of cardiac parasympathetic neurons in the nucleus ambiguus. *Neuroscience* 111**,** 699-705.

Waters, J.C. (2009). Accuracy and precision in quantitative fluorescence microscopy. *J. Cell Biol.* 185**,** 1135-1148.

White, J.D., Krause, J.E., and Mckelvy, J.F. (1984). In vivo biosynthesis and transport of oxytocin, vasopressin, and neurophysins to posterior pituitary and nucleus of the solitary tract. *J. Neurosci.* 4**,** 1262-1270.

Wright, J.W., and Harding, J.W. (2013). The brain renin-angiotensin system: a diversity of functions and implications for CNS diseases. *Pflugers Arch.* 465**,** 133-151.

Wu, X., Kihara, T., Hongo, H., Akaike, A., Niidome, T., et al. (2010). Angiotensin receptor type 1 antagonists protect against neuronal injury induced by oxygen–glucose depletion. *Br. J. Pharmacol.* 161**,** 33-50.

Xu, B., Zheng, H., Liu, X., and Patel, K.P. (2015). Activation of afferent renal nerves modulates RVLM projecting PVN neurons. *Am. J. Physiol. Heart Circ. Physiol.***,** H1103-1111.

Yao, Y., Hildreth, C.M., Farnham, M.M., Saha, M., Sun, Q.J., et al. (2015). The effect of losartan on differential reflex control of sympathetic nerve activity in chronic kidney disease. *J. Hypertens.* 33**,** 1249-1260.

Ye, S., Zhong, H., Yanamadala, S., and Campese, V.M. (2006). Oxidative stress mediates the stimulation of sympathetic nerve activity in the phenol renal injury model of hypertension. *Hypertension* 48**,** 309-315.

Zhang, Y., Yu, Y., Zhang, F., Zhong, M.K., Shi, Z., et al. (2006). NAD(P)H oxidase in paraventricular nucleus contributes to the effect of angiotensin II on cardiac sympathetic afferent reflex. *Brain Res.* 1082**,** 132-141.

Zhu, G.Q., Zucker, I.H., and Wang, W. (2002). Central AT1 receptors are involved in the enhanced cardiac sympathetic afferent reflex in rats with chronic heart failure. *Basic Res. Cardiol.* 97**,** 320-326.

Ziegler, D.R., Edwards, M.R., Ulrich-Lai, Y.M., Herman, J.P., and Cullinan, W.E. (2012). Brainstem origins of glutamatergic innervation of the rat hypothalamic paraventricular nucleus. *J. Comp. Neurol.* 520**,** 2369-2394.

Zimmerman, M.C. (2011). Angiotensin II and angiotensin-1-7 redox signaling in the central nervous system. *Curr. Opin. Pharmacol.* 11**,** 138-143.

Zimmerman, M.C., Dunlay, R.P., Lazartigues, E., Zhang, Y., Sharma, R.V., et al. (2004). Requirement for Rac1-dependent NADPH oxidase in the cardiovascular and dipsogenic actions of angiotensin II in the brain. *Circ. Res.* 95**,** 532-539.

Zimmerman, M.C., Lazartigues, E., Lang, J.A., Sinnayah, P., Ahmad, I.M., et al. (2002). Superoxide mediates the actions of angiotensin II in the central nervous system. *Circ. Res.* 91**,** 1038-1045.

Zittema, D., Van Den Berg, E., Meijer, E., Boertien, W.E., Muller Kobold, A.C., et al. (2014). Kidney function and plasma copeptin levels in healthy kidney donors and autosomal dominant polycystic kidney disease patients. *Clin. J. Am. Soc. Nephrol.* 9**,** 1553-1562.

MACQUARIE University ANIMAL RESEARCH AUTHORITY (ARA)

AEC Reference No.: 2015/001 -3 **Date of Expiry:** 23 February 2016

***Full Approval Duration:** 23 February 2015 to 21 February 2018 (36 months)*

This ARA remains in force until the Date of Expiry (unless suspended, cancelled or surrendered) and will only be renewed upon receipt of a satisfactory Progress Report before expiry (see Approval email for submission details).

Principal Investigator:
Professor Jacqueline Phillips
School of Advanced Medicine
Macquarie University, NSW 2109
jacqueline.phillips@mq.edu.au
0409 225 707

Associate Investigators:
Cara Hildreth 0412 266 420
Research Asisstant:
Rochelle Boyd 0409 322382
Student:
Sheran Li 0452 395 550
Connor Underwood 0430 882 545

In case of emergency, please contact:
the Principal Investigator / Associate Investigator named above
or Manager, CAF: 9850 7780 / 0428 861 163 and Animal Welfare Officer: 9850 7758 / 0439 497 383

The above-named are authorised by MACQUARIE UNIVERSITY ANIMAL ETHICS COMMITTEE to conduct the following research:

Title of the project: Plasticity in the brain driving impaired heart rate reflex function in chronic kidney disease
Purpose: 4 - Research: Human or Animal Biology

Aims: To investigate the role of long-term altered brain signalling (plasticity) in the development of baroreflex dysfunction in the Lewis Polycystic Kidney disease rat model of chronic kidney disease

Surgical Procedures category: 5 - Major Surgery with Recovery
All procedures must be performed as per the AEC-approved protocol, unless stated otherwise by the AEC and/or AWO.

Maximum numbers approved (for the Full Approval Duration):

Species	Strain	Age/Weight/Sex	Total	Supplier/Source
02 Rattus	Lewis	3 to 14 weeks /NA/Any	106	Animal Resources Centre Perth Western Australia
02 Rattus	Lewis Polycystic Kidney	3 - 14 weeks/NA/Any	106	Animal Resource Centre Perth Western Australia
			212	

Location of research:

Location	*Full street address*
Central Animal Facility	Building F9A, Research Park Drive, Macquarie University, NSW 2109
School of Advanced Medicine	Level 1, F10A, 2 Technology Place, Macquarie University, NSW 2109

Amendments approved by the AEC since initial approval:
1. Amendment #1: Amend experimental design *(combining two steps of currently approved protocol)*, Exec approved, ratified by AEC 16 April 2015)
2. Amendment #2: Amend technique/procedure (Exec approved, ratified by AEC 14 May 2015).

Conditions of Approval:
1. Amendment #2: Amend technique/procedure - ***The AEC has requested that the Researcher provide a report regarding post-operative outcomes using both drugs and report back to the next AEC meeting on 18 June 2015.***

Being animal research carried out in accordance with the Code of Practice for a recognised research purpose and in connection with animals (other than exempt animals) that have been obtained from the holder of an animal suppliers licence.

Professor Mark Connor (Chair, Animal Ethics Committee) **Approval Date: 14 May 2015**

Adapted from Form C (issued under part IV of the Animal Research Act, 1985)